TUM

Optimizing Siting of Urban Air Mobility Vertiports in Multimodal Transportation Networks with Two-Stage Stochastic Programming

A thesis presented in part fulfilment of the requirements of the Degree of Master of Science in Transportation Systems at the Department of Mobility Systems Engineering, Technical University of Munich.
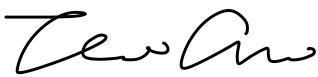
Supervisor   M.Sc. Hao Wu

                        M.Sc. Qing-Long Lu

                        Univ.-Prof. Dr. Constantinos Antoniou

                        Chair of Transportation Systems Engineering

Submitted by   Tao Guo

Submitted on   Munich, 16.01.2024

Declaration

I hereby confirm that the presented thesis work has been done independently and using only the sources and resources as are listed. This thesis has not previously been submitted elsewhere for purposes of assessment.

München, 16.01.2024, Signature

Acknowledgements

My journey into the field of Urban Air Mobility began a year ago during a project seminar. This exploration, encompassing the impact of UAM on accessibility, siting of UAM vertiports through clustering methods, and optimization strategies for vertiport locations, culminates in this thesis. This work, marking the finale of my master's studies, has condensed a lot of our efforts.

I am profoundly grateful to my supervisor, Hao Wu, for introducing me to the fascinating world of UAM. Our numerous collaborations over the past year have not only enriched my knowledge but also imbued me with the quintessential qualities of a researcher. The origin of this thesis stems from his innovative ideas, supported by his deep expertise in UAM and MATSim. His patience and guidance, especially during challenging phases of my research, have been invaluable. The solutions to many problems I encountered emerged through our enlightening discussions, and his mentorship during the thesis writing process has been irreplaceable.

My heartfelt thanks also go to my co-supervisor, Qing-Long Lu. His assistance in developing the optimization model and the inspiration to apply the two-stage stochastic optimization model were crucial. His profound understanding of optimization theory greatly facilitated my research. Furthermore, his tireless efforts and detailed feedback in revising my thesis are deeply appreciated.

I extend my sincere appreciation to my mentor, Prof. Dr. Constantinos Antoniou. His guidance was pivotal at critical junctures of my research. The adjustments made based on his insightful comments significantly shaped my work. His valuable suggestions during the thesis revision process were dramatically beneficial.

Lastly, but most importantly, I owe a world of gratitude to my parents, Qing-Song Guo and Juan Wei. Their unwavering love, support, and belief in my aspirations have been my pillars of strength. Their encouragement and financial support were the bedrock of my decision to study abroad three years ago. Their belief in my dreams and aspirations has been a constant source of motivation and strength.

Abstract

Urban Air Mobility (UAM) represents an emerging mode of transportation, garnering significant research interest due to its potential to reduce travel time notably. The strategic selection of vertiport locations critically influences the effectiveness of UAM services. Initial studies on UAM vertiport siting primarily utilized existing infrastructure, Multi-Criteria Decision Analysis (MCDA) based on expert opinions, clustering methods, and optimization methods. Among these, optimization methods are preferred for their efficiency, generalizability, and ability to ensure optimal solutions. However, previous research using optimization for UAM vertiport siting has largely overlooked the stochastic nature of travelers' mode choice, particularly in the context of disaggregated demand data. This study formulates the vertiport siting problem as a two-stage stochastic optimization problem by considering mode choice to address the above research gap. In the designed framework, the first-stage decision involves selecting the most appropriate vertiport locations from the vertiport candidates (siting), and the second-stage decision entails pairing each trip with the optimal access and egress vertiports (matching). This study developed and employed heuristic approaches to solve the optimization problem based on the above facts.

Utilizing the proposed framework, the case study was designed to select 74 vertiports from 200 candidates, aiming to maximize the total saved generalized travel costs across all trips within the Munich metropolitan area (MUC), Germany. Notably, Greedy Forwards-Update (GRDF-U), Genetic Algorithm (GA), and Simulated Annealing (SA) yielded remarkably similar and superior outcomes regarding optimization efficacy, demand coverage, and accessibility improvement. All optimization-based solutions outperformed benchmarks from previous studies using MCDA and clustering methods in terms of saved generalized costs. Additionally, an exploratory experiment on the impact of vertiports' numbers was also conducted. The results indicate that saved generalized travel costs continue to increase as the number of vertiports increases but exhibit diminishing marginal returns. In contrast, construction costs almost linearly increase. This proves that building excessive vertiports is not a sensible endeavor.

Contents

List of Figures

List of Tables

Glossary

A

C

D

E

G

H

K

M

N

1. Introduction

1.1. Background

As modern cities continue to expand and evolve, they encounter a significant and multi-faceted problem in transportation. This issue is chiefly characterized by escalating congestion and inadequate infrastructure. Urban sprawl, a common feature in rapidly growing metropolitan areas, exacerbates the issue by stretching transportation networks to their limits and beyond. This expansion invariably results in longer commutes, putting excessive strain on existing roads and public transit systems that were not designed to handle such high volumes of traffic or such vast geographic coverage. At present, there exists a wealth of research focused on mitigating traffic congestion. Broadly, these efforts can be categorized into two domains: transportation demand management (TDM) and transportation system management (TSM), in accordance with classical traffic theories (Meyer, 1999). The former seeks to reduce private traffic demand through enhanced land-use planning (e.g., the concepts of 15-minute city (Moreno et al., 2021)) or modal shifts (e.g., promoting the use of public transport (Cullinane, 2002)). The latter employs various traffic control measures (e.g., traffic signal control (Mirchandani and Head, 2001), high-occupancy vehicle lanes for carpooling (Hanna et al., 2017)) to optimize the operation efficiency and carrying capacity of the transportation system. However, as highlighted by Wang and Qu (2023), such measures failed to address the underlying contradiction between rising traffic demand, limited land use, and the capacity constraints of road transport. Consequently, some have shifted their perspective to the realm of airspace.

Recent technological advancements, including battery and fuel cell electric vehicles, autonomous vehicles, and unmanned aerial vehicles (UAVs), have brought about rapid transformations in the field of transportation (Biswas et al., 2021). Urban Air Mobility (UAM) emerges as a nascent airborne transportation concept, typically involving on-demand, station-based, inter- and intra-urban passenger transportation services facilitated by electric vertical takeoff and landing (eVTOL) aircraft (conceptual design shown in Figure 1). UAM holds the potential to become a competitive mode of passenger transportation, offering safer, more efficient, and sustainable travel options (Rothfeld, 2021).

Existing research highlights numerous economic benefits and opportunities stemming from the integration of UAM into existing transportation systems. Tuchen et al. (2022) qualitatively asserted that UAM development could stimulate job creation through the manufacture of aircraft-related materials and vertiport construction. Moreover, both business and community development could be amplified, especially in the vicinity of manufacturing centers and vertiports. Numerous studies have also explored the potential of UAM as a solution for freight transportation (Gunady et al., 2022; Li et al., 2022). These studies collectively sug-

Figure 1 Conceptual design of UAM aircraft (Technische Hochschule Ingolstadt, 2022).

gest that UAM could revolutionize the logistics industry, primarily due to its rapid and efficient transport capabilities. UAM could potentially ease the transportation of goods to remote areas, which are often inaccessible via conventional transportation modes. Furthermore, UAM holds promise in providing high-performance services for emergency traffic or commuting between rural, suburban, and urban areas, thus enhancing citizens' accessibility (Pukhova et al., 2021). However, consensus remains elusive regarding whether UAM introduction can effectively alleviate traffic congestion. Pukhova et al. (2021) contended that, when accounting for access and egress legs to UAM stations, total car travel kilometers increased by 0.3%, casting doubt on UAM's ability to reduce traffic congestion effectively. Wang and Qu (2023) further noted that modal shifts to UAM could intensify ground travel demands near vertiports, exacerbating congestion in those areas. Kellermann et al. (2020) acknowledged that a substantial reduction in traffic remains elusive due to the technological limitations of UAVs, suggesting that redistribution of traffic is a more likely outcome, offering the potential to alleviate congestion. Doole et al. (2018) conducted simulations in the Paris metropolitan area, concluding that if eVTOL aircraft traffic reached 180,000 flights per hour, it would be possible to divert 70% of ground traffic to the air. Despite some controversies, the positive impact of UAM on existing transportation systems and regional economic development is undeniable. Maximizing the benefits of UAM involves multiple aspects, including planning, design, and operation. Among these, the siting of UAM vertiports is a critical component.

1.2. Motivations

The performance of UAM service is influenced by various parameters, including the number and location of vertiports, speed, number of seats, and passenger processing time (Ploetner et al., 2020). The placement of UAM vertiports is a pivotal factor that has undergone extensive study, demonstrating its substantial impact on both UAM demand and accessibility (Ploetner et al., 2020). According to Liu et al. (2023), the establishment of an adequate

number of vertiports and meticulous site planning are crucial for facilitating efficient and sustainable UAM system operations. For instance, Guo et al. (2024) stated proper vertiport siting not only enhances the transport efficiency but also the accessibility of the UAM system. On top of that, as with any other public facility site selection, once a vertiport location has been established, it cannot be easily changed again for a considerable period, and re-siting often means rebuilding the infrastructure, which is quite expensive. Lim and Hwang (2019) underscored that the feasibility of UAM is more determined by the location of vertiports than their number, especially when integrated with public transport. Furthermore, from the operator's perspective, Onat et al. (2023) indicated that the distance between vertiports is a crucial factor influencing fleet utilization, i.e., sparse vertiports siting results in reduced total idle time and increased cruise and charge times, leading to more efficient fleet utilization but also longer passenger delays. Consequently, the selection of vertiport locations is critical from both UAM service performance and cost perspectives. Therefore, a comprehensive consideration of UAM vertiport siting is crucial for realizing the full potential of the UAM system. This study introduces a generic method for UAM vertiport siting using a two-stage stochastic optimization approach with the objective of maximizing cost savings for all trips. Given a set of potential vertiport candidate locations and the desired number of vertiports, the algorithms can identify at least an approximate optimal solution for vertiport siting.

1.3. Contributions

This study's first contribution lies in formulating the choice of vertiport locations as a two-stage stochastic optimization problem. This framework proposes the expression of an individual's mode choice through a series of binary stochastic variables. In this study, individual mode choices are determined by employing Monte Carlo sampling, in which probabilities are computed by using discrete choice models. This approach encompasses both utility-based and stochastic behavioral aspects of travelers' mode choices and could provide a more reliable mode choice estimation.

The second major contribution of this study lies in the development of two heuristic algorithms for the large-scale network optimization problem. This study used five heuristic algorithms in the first-stage optimization, of which the Greedy Forwards Update (GRDF-U) Algorithm and Greedy Backwards (GRDB) Algorithm are constructed by the authors themselves. Moreover, the experiment results show that GRDF-U yields superior performance regarding the optimization solution, which is comparable with the GA and SA solutions. GRDB delivers the most efficient computation time while still achieving satisfactory optimization outcomes.

Lastly, from a policy development perspective, this study introduces a universally applicable method, even in cases where expert support is limited, and data is scarce. It enables the fool-proof selection of optimal (or near-optimal) vertiport locations based on predefined objectives, which yields excellent performances concerning saved generalized travel cost, demand coverage, and accessibility improvement, compared with benchmarks. Additionally,

the exploratory study qualitatively analyzes the trade-off between the number of vertiports and the associated benefits and costs. The marginal diminishing benefit effect of vertiports' number is verified. When future cost estimations become more precise, determining the optimal number of vertiports can be conveniently incorporated into the formulation of this study.

1.4. Thesis Structure

The remainder of this thesis is structured as follows: Chapter 2 critically reviews existing research concerning factors influencing vertiport location selection and approaches for vertiport siting. Before delving into the methodology of this thesis in detail, Chapter 3 proposes the procedures of two alternative vertiports siting approaches, namely MCDA and clustering. Chapter 4 and 5 delineate the key assumptions, problem formulations, and procedures for model choice modeling, demand allocation optimization, and the utilization of heuristic algorithms for vertiport siting optimization. Chapter 6 outlines the design and configuration of the experiment, which is followed by the presentation and thorough analysis of the results in Chapter 7. Subsequently, the limitations and directions for future research are discussed and highlighted in Chapter 8. The study concludes in Chapter 9, providing a summary of the study's findings as well as policy insights for UAM network planning based on the findings.

2. Literature Review

2.1. Overview of Vertiports Siting Related Studies

The choice of vertiport locations, often referred to as vertiport siting, represents a substantial and pivotal challenge in the successful implementation of UAM. Consequently, this aspect has garnered significant attention within the realm of UAM research. As demonstrated by a systematic review of UAM-related literature conducted by Schweiger and Preis (2022), the selection and establishment of vertiport locations, as well as the development of associated networks, constitute a substantial portion of all UAM ground infrastructure publications. A subset of these studies concentrates on identifying the factors that influence the selection of vertiport locations, while others introduce innovative methods for siting. Nearly all of them rely on case analyses. Before delving into the methodological aspects of these studies, it is valuable to examine the geographic distribution of the regions selected for these case analyses. Figure 2 indicates the locations chosen for case studies in recent years concerning UAM vertiport siting. On a global scale, Europe, the United States, and South Korea emerge as the primary focal points for vertiport location research. More precisely, multiple case analyses have designated Munich, Seoul, San Francisco (Northern California), Los Angeles, and New York as their primary study areas. These regions share a common trait of being economically developed with a high level of resident income (The World Bank, 2022). This aligns with the prevailing consensus in previous research, which suggests that UAM is generally better suited for populations with higher income levels (Ploetner et al., 2020).
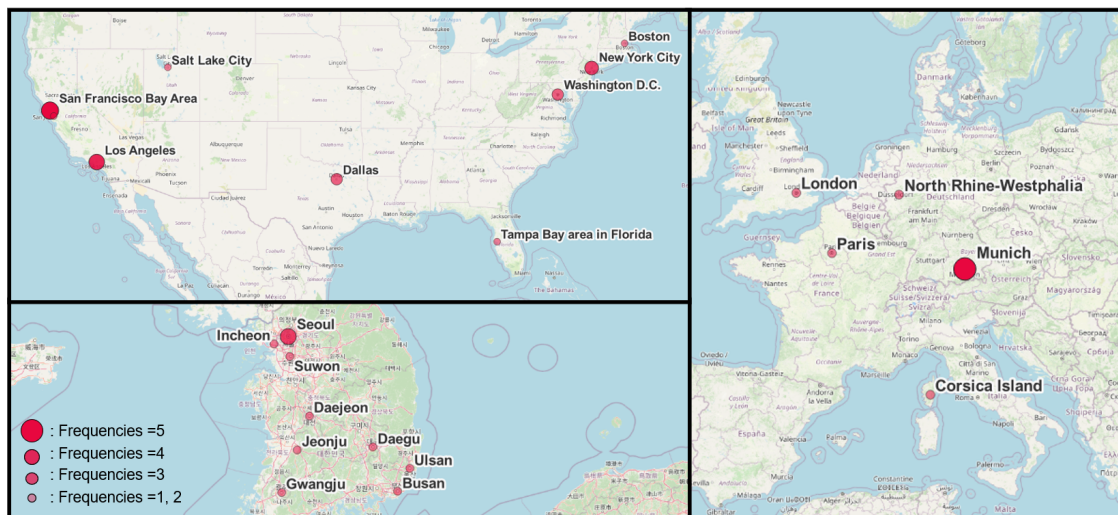
Figure 2 Distribution of UAM vertiport siting case studies around the world.

Understanding the factors that impact the selection of vertiport locations is equally imperative. Fadhil (2018) identified ten factors that could influence the placement of UAM ground infrastructure, taking into account both demand-side factors (population density, median in-

Figure 3 Word cloud of UAM vertiports siting's influencing factors.

come, office rent prices, points of interest, major transportation hubs, annual transportation costs, job density, and extreme commuting) and supply-side factors (existing infrastructures and noise). These factors are prioritized by experts in his study, in which points of interest, major transport nodes, and median income are the top 3 factors of concern. Based on the work of Fadhil (2018), Arellano (2020) supplemented several factors that would have a significant impact on the location of UAM vertiports, namely company headquarters, travel demand, and accessibility. Similarly, a review of recent air taxi developments by Rajendran and Srinivas (2020) highlighted key factors contributing to a location being chosen as a UAM vertiport, which can be summarized as follows: demand density, the availability of adequate space for safe takeoff and landing, the presence of suitable areas for charging facilities, and ease of accessibility. Figure 3 shows a word cloud created from the factors mentioned in these contributions. The size of the font depends on the frequency of occurrence. It is clear that **Density** (indicating population density, job density, employment density), **Existing** (helipads, infrastructure, facilities), **Accessibility** (indicating opportunity accessibility, UAM station accessibility), and **Demand** (indicating travel demand, UAM demand, demand inducement) are the words that stand out from the crowd. In short, most scholars agree that UAM Vertiport siting is primarily demand-oriented and aims to improve residents' accessibility while integrating with existing infrastructure.

Based on the consideration of these factors, various valuable efforts have been made in recent years to identify suitable UAM vertiport locations. Prior studies have utilized a wide array of both qualitative and quantitative methods to determine optimal locations for UAM stations. The former is represented by the direct use of existing infrastructure and Multi-Criteria Decision Analysis (MCDA), and the latter includes clustering and optimization-based methods.

2.2. Qualitative Vertiports Siting Approaches

In the early stages of UAM-related research, when the factors influencing station location determination were not yet extensively explored, mainstream studies often recommended the utilization of existing infrastructure as potential vertiport sites. For instance, Antcliff et al. (2016), after analyzing the characteristics of existing infrastructure and airspace regulations in Silicon Valley, USA, proposed the use of water barges, highway cloverleaf interchanges, and private tech business campuses as suitable vertiport locations in bay-surrounding areas, urban settings, and private land-use areas, respectively. Similarly, in North Rhine-Westphalia, Germany, Otte et al. (2018) suggested repurposing existing passenger, public, and special-purpose airfields as UAM stations, while also considering adequately sized rooftops within densely populated areas as potential UAM vertiport locations. Additionally, Vascik (2017) explored the possibility of available takeoff and landing areas (TOLAs) in conjunction with other infrastructures besides helipads as eVTOL Aircraft's technology evolves further. For instance, when considering reduced downwash effects or vehicles certified for landing on smaller footprints, these TOLAs could be strategically co-located in gas stations, superstores, or other geographically well-distributed businesses. This approach offers the advantage of minimizing the construction cost of UAM ground infrastructure and is well-suited for short- to medium-term UAM planning.

MCDA is a decision-making approach that involves evaluating and comparing multiple criteria or factors when making decisions (Lloyd-Williams and Lloyd-Williams, 2019). It is particularly useful when decisions need to be made based on multiple, and sometimes conflicting, criteria or objectives. In the context of UAM vertiport placement, more comprehensive approaches that consider a multitude of factors, especially those related to demand, have been employed. For example, Fadhil (2018) presented a methodology for strategically placing UAM vertiports in the Metropolitan areas of Los Angeles, USA, and Munich, Germany, using a Geographic Information Systems (GIS)-based approach. The study employed the weighted linear combination (WLC) technique to conduct a suitability analysis, identifying appropriate areas for UAM vertiports. The minimum requirements and influential factors were determined through a literature review. Weightings for each factor were generated using an analytic hierarchy process (AHP)-Delphi method, along with interviews with "super-experts". The resulting suitability maps highlighted areas with high scores in city centers, major transport hubs, and densely populated, high-income regions. In another case study by Ploetner et al. (2020) in the Upper Bavaria Region, Germany, potential vertiport locations were determined through workshops involving representatives from Munich Airport, the city of Munich, Ingolstadt, and the Upper Bavarian Chamber of Industry and Commerce. This process considered four main trip purposes: commuting, business, tourism, and leisure. The research proposed three levels of vertiport archetypes: a low-density network with 24 vertiports covering large agglomerations, transport hubs, and densely populated areas with a higher income; a medium-density network with 74 vertiports, including underground and suburban line stations and employment areas; and a high-density network covering all rele-

vant trips and groups. Similarly, Arellano (2020), focusing on the same study area as Fadhil (2018) and Ploetner et al. (2020), employed a demand-based approach to determine UAM vertiport locations. It developed a semi-automated procedure using a GIS multi-criteria decision analysis framework. Like the study by Fadhil (2018), influential factors for UAM vertiport locations were collected and prioritized. The station allocation aimed to maximize coverage for all demand points. The network's performance was assessed by comparing UAM demand and travel times to ground transportation and manually selected networks in the Oberbayern Urban Air Mobility (OBUAM) project by Ploetner et al. (2020). The results indicated higher UAM demand, but less time savings compared to manual networks. Both demand and travel time savings were found to be influenced by geographical distribution and the effective placement of vertiports.

Reviewing the methodologies and results of studies employing MCDA in UAM vertiport siting, it becomes evident that MCDA offers advantages of effective integration with land-use patterns, consideration of multiple criteria, and stakeholder engagement. However, it also has drawbacks, including a reliance on experts' opinions, which may not be feasible in all regions and can overly introduce subjectivity into the decision-making process.

Furthermore, some researchers have proposed specialized approaches that integrate the UAM network planning with the city's land-use patterns and geographic features. For instance, Patterson et al. (2018) observed that many cities in the USA exhibit a "wheel-and-spoke" configuration with beltways and highways, offering valuable insights for UAM network design. Consequently, they developed a hexagonal model for the UAM network, where vertiports are strategically positioned at the vertices of the hexagons. This model can be expanded by adding equilateral triangles or individual vertiports around the inner hexagon. The primary advantage of this approach lies in maintaining a consistent distance between any two adjacent vertiports, enabling efficient mobility across the city. However, this equilateral hexagonal UAM network is overly idealized and difficult to realize in developed areas where site planning is already complete. In addition, it does not take UAM demand into account and is difficult to apply in practice.

2.3. Quantitative Vertiports Siting Approaches

A commonly used quantitative approach for determining UAM vertiport locations is clustering, a widely used machine learning and data analysis technique for grouping similar data points or objects based on their inherent characteristics or features. The general methodology for using clustering in vertiport siting involves taking demand locations as data points and performing clustering on these points. The centroids of clusters are then considered as potential vertiport locations.

For example, Syed et al. (2017) treated census tract population centroids in Northern California and Washington D.C., USA as demand points and weighted them based on population

income. They applied K-means clustering to identify suitable UAM station locations. Similarly, Lim and Hwang (2019) used K-means clustering for the origins of commute trips in Seoul, South Korea. After implementing the simulation with NAVER Direction, the travel time savings for the three most demanding routes were calculated to evaluate UAM vertiport siting results. In a study focused on New York City, USA, Rajendran and Srinivas (2020) considered taxi demand as potential demand points for UAM and applied a variant of K-means clustering. This variant included two constraints: one constraining the total distance of demand points to their cluster centroids and the other setting a threshold for demand fulfillment. Evaluation criteria in their research included the Davies-Bouldin index, travel time savings, passengers' willingness to fly, and demand fulfillment rate. As a follow-up study to Lim and Hwang (2019), Jeong et al. (2021) further explored UAM vertiport selection in Seoul, South Korea, using K-means clustering with residential locations of commuting populations as demand points. They employed the Silhouette technique to evaluate clustering results. As the first study highlighted the effects of initialization in employing K-means clustering, Bulusu et al. (2021) chose K-means++ techniques in their research by taking origins and destinations of cross-bay commute trips in San Francisco Bay Area, USA. They employed SF-CHAMP for a more realistic traffic simulation, and accordingly, travel time savings and demand shift were chosen as evaluation metrics. While most of the above studies utilized K-means clustering and its variants, Guo et al. (2024) utilized five clustering methods from different clustering categories, namely K-means (KM) (++) clustering, Gaussian mixture model (GMM) clustering, mean shift (MS) clustering, hierarchical clustering (HC), and density-based spatial clustering of applications with noise (DBSCAN) clustering, to locate UAM vertiports in the Munich metropolitan area, Germany. They used residential addresses as demand points and employed Multi-Agent Transport Simulation (MATSim) to calculate travel time savings and accessibility improvements.

Methods based on clustering for determining UAM vertiport locations are straightforward and effectively consider potential UAM demand. Additionally, these methods are easily generalizable. However, these methods cannot guarantee optimal solutions in general. Moreover, factors such as land-use characteristics can be challenging to incorporate during the clustering process. Besides, some clustering methods are highly sensitive to initialization, which can result in relatively low robustness of outcomes.

Another commonly used method for determining vertiport locations is optimization. The vertiport siting problem is often viewed as a variant of the classic hub location problem (HLP) (Willey and Salmon, 2021). HLP involves identifying the optimal locations for hub facilities from a list of candidates, such as warehouses, distribution centers, or airports, in a network to minimize transportation costs and enhance the efficiency of goods distribution (O'kelly, 1987). Depending on the specific objectives and constraints, HLP can be categorized into different variants, including the p-Hub Location Problem, p-Hub Median, p-Hub Center, and p-Hub Maximal Covering Location Problem (Farahani et al., 2013).

In the classical p-Hub Location Problem, the number of hubs is determined exogenously and denoted by p. Every two hub nodes are directly connected. Each non-hub node is linked to a single hub node, meaning that for a trip between non-hub nodes, at least one and at most two hub nodes must be traversed. The objective is to minimize the total transportation cost between network nodes. This model was originally proposed and formulated by O'kelly (1987). The p-Hub Location Problem is quadratic because a non-hub node can be allocated to a hub node only when a hub is located at that node. This constraint is relaxed in the p-Hub Median Location Problem, which allows multiple allocations of non-hub nodes and leads to a linear mathematical formulation (Campbell, 1996). Originally introduced by Campbell (1994), the p-Hub Center Location Problem has similar assumptions and constraints as the p-Hub Median but focuses on minimizing the maximum transportation cost from origin nodes to destination nodes. Due to this nature, it finds wide applications in emergency facility location problems (Farahani et al., 2013). The p-Hub Maximal Covering Location Problem, also proposed by Campbell (1994), shares similar assumptions and constraints with the p-Hub Median and Center problems but aims to maximize the amount of transportation demand covered by the p hubs. In this model, origin-destination (OD) pairs are considered covered only if there are hub facilities within their predefined distance. Existing research on determining UAM vertiport locations using optimization methods typically relies on one of the aforementioned models.

As a seminal work in the field, Holden and Goel (2016) formulated the vertiport siting problem as a p-Hub Maximal Covering location problem with the objective of maximizing the total trip coverage of long-distance riders. They first employed K-means clustering on the origins and destinations of long-distance trips to identify potential vertiport candidates. Then they used integer programming to solve the above-mentioned optimization problem. The UAM demand is obtained by adding a constraint that at least a 40% time saving could be achieved by UAM service. With the objective of maximizing potential cumulative population time savings compared with driving, Daskilewicz et al. (2018) used aggregate travel data in San Francisco and Los Angeles, USA, and found the optimal vertiport locations from the census tracts, which are treated as vertiport candidates. It is the first attempt at UAM network optimization with the objective of time-saving; however, the uncertainty in mode choice behavior was overlooked in their study. The potential UAM demand was constrained within the trips whose origin and destination are in the catchment area of vertiports. Besides, the UAM traveling time was not counted for access and egress legs, which could considerably deviate from reality. Rothfeld et al. (2021) combined evenly spaced grid points and expert-placed potential vertiport locations in Munich, Germany, as the candidate hub locations and formulated the vertiport siting problem as a p-median problem with an objective of minimizing the weighted travel time impedance between all zone centroids and vertiports. The weight was determined by the aggregate travel demand of each zone. ESRI's location-allocation tool was used in their study to solve the optimization problem. Subsequently, Wu and Zhang (2021) also formulated the problem as a p-median problem that aims to minimize the generalized travel cost of all trips using integer programming. Different from Daskilewicz et al.

(2018) and Rothfeld et al. (2021), the travel data in their research were disaggregated and represented the long-distance trips in Tampa Bay Area, USA. According to Wu and Zhang (2021), the objective of minimizing generalized cost is equivalent to maximizing the saved generalized cost brought by UAM service, which has provided a basis for many studies. In this way, vertiport candidates were derived by dividing the study area into hexagonal grids, followed by manual removal of unsuitable land-use areas and merging adjacent ones, significantly reducing the number of candidates. Nonetheless, in the new formulation, mode choice is usually treated as a decision variable with a constraint to ensure that UAM can generate a positive generalized travel cost saving, indicating that the mode choice for individual trips will always be optimized in a direction that minimizes the generalized travel cost. Unfortunately, this assumption overlooks the stochastic nature of mode choice behaviors, leading to an overestimation of the cost-saving effects of UAM. Willey and Salmon (2021) addressed the vertiport selection problem by framing it as a modified single-allocation p-hub median location problem, aiming to minimize travel time for all trips. This approach integrates subgraph isomorphism elements to develop structured networks suitable for public transit operations. Vertiport candidates were identified from existing airports and helipads, enhanced by potential locations identified through DBSCAN clustering. The study focused on three city pairs within the USA for its experiment. To tackle the NP-hard nature of the problem, four heuristic algorithms were utilized. However, the research's travel demand, aggregated as zonal OD pairs, limited the individual mode choice representation. The probability of choosing UAM trips for an OD pair was determined by the minimum willingness to travel to hub nodes (vertiports) connected to the respective ODs. This model, reliant on drive time, oversimplifies the mode choice aspect since willingness to travel varies individually. Wang et al. (2022) developed an integrated framework to maximize the efficiency and profitability of UAM operations. This framework uniquely captures the interdependence among strategic vertiport planning, tactical UAM operations, and passenger demand. Furthermore, to address the multi-level complexity of the optimization problem, the authors introduced an adaptive discretization algorithm. The study utilized aggregated travel demand data from New York City, Boston, Dallas, and San Francisco, USA, for its numerical experiments. The mode choice analysis in their study was conducted using a multinomial logit (MNL) model combined with distributional robust optimization. However, while the model effectively solves for the "end-state" network, it falls short in addressing dynamic network expansions. Rath and Chow (2022) developed two distinct optimization models targeting separate objectives: one to maximize the ridership of air taxis and another to maximize the revenue. Employing linear programming techniques, these models were designed to select optimal skyport locations from the 149 taxi zones in New York City, USA. The study primarily focused on taxi trips to and from airports, utilizing a binary logit model to predict the shift in mode choice from traditional taxi services to air taxis. This integration of a discrete choice model into the network optimization highlighted the complexities of modeling user behavior in such problems. However, a key limitation identified was the binary logit model's assumption that modal shifts occur exclusively from taxis to air taxis. Building upon Rath and Chow (2022)'s work, He et al. (2023) introduced the hierarchical optimization method (HOME), significantly enhancing the computational speed

of integer programming. This method was validated through a case study conducted in Los Angeles, USA, demonstrating its effectiveness.

The optimization problems mentioned above all pertain to single optimization objectives. Nevertheless, there are also models that incorporate multiple optimization objectives within a single framework. Boo et al. (2023) employed the ϵ-constraint method to formulate a multi-objective optimization model. Their objective was to maximize the accessibility of vertiports to tourist attractions, transportation hubs, and commercial centers, while simultaneously minimizing the overall cost of land acquisition and the total aerial distance between vertiports. They substantiated the practicality of this optimization model by utilizing nine major cities in South Korea, including Seoul and Busan, as illustrative instances for the siting of vertiports. Similarly, Brulin and Olhofer (2023) formulated an optimization model with the primary aim of maximizing the demand covered by UAM vertiports while concurrently minimizing the count of vertiports required. To accomplish this, they devised a bi-network comprising two layers of loops. In the outer layer loop, the Pareto-optimal non-dominated sorting genetic algorithm (NSGA-II) method was employed to pinpoint the optimal locations for UAM vertiports. Meanwhile, the inner layer loop made use of MATSim's proprietary algorithm, namely, the co-evolutionary algorithm (CEA), to adapt the plans of individual agents to reflect changes in travel behavior following the implementation of UAM (Horni et al., 2016). Remarkably, this paper stands as a unique contribution in the field, as it integrates MATSim with UAM network optimization. However, a conspicuous issue arises in which the inner layer optimization objective seeks to maximize the total score of all agents' trips and activities, a goal that is incongruent with the objective of the outer layer optimization. As acknowledged by the authors, the actual purpose of the inner layer loop is to reassess the network design, a fact that may appear somewhat perplexing.

Since the research regarding optimization-based vertiports siting is intimately related to this study and there are more points to focus on, all the related studies using optimization methods to site vertiports are summarized again in Table 1 in order to show a clearer presentation of the methodologies provided by the past studies as well as their contributions and limitations. Here, the optimization objective, the consideration of the vertiport's capacity, the solution of the optimization problem, the type of demand (i.e., aggregate or disaggregate), how mode choice is modeled, and how candidates are identified are the core issues of concern. Furthermore, the proposed methodologies and considerations in this study are highlighted in the last row of Table 1 for comparison.

Table 1 Summary of literature review on optimization vertiports siting approach.

Paper	Objective	Vertiport's Capacity	Solution Approach	Travel Demand	Mode Choice	Vertiport Candidates	Innovative Points	Limitations
Holden and Goel (2016)	Maximize the total trip coverage of long-distance riders.	Uncapacitated	Integer programming	Disaggregate	Objective of the problem. Constraint: 40% time saving.	K-means clustering	Categorize UAM ground infrastructures as vertiports and vertistops. Use K-means clustering to identify vertiports candidates.	Constraint of 40% time saving for UAM trips is too simplistic.
Daskilewicz et al. (2018)	Maximize cumulative population time-saving compared with driving.	Uncapacitated	Integer programming	Aggregate	Constraints by catchment area of each vertiport. No mode choice consideration.	Each census tract could be a candidate vertiport location.	The first attempt of UAM network optimization with the objective of time-saving.	UAM traveling time is not counted for access/egress legs. No consideration of mode choice.
Rothfeld (2021)	Minimize the weighted travel time impedance between all zone centroids and vertiports. Weight: aggregated trips.	Uncapacitated	ESRI's location-allocation tool	Aggregate	No consideration of mode choice	Combine evenly spaced grid points and experts placed potential vertiport locations.	Utilize ESRI's location-allocation tool.	Aggregated demand might be distorted. No consideration of mode choice.
Wu and Zhang (2021)	Maximize the saved generalized travel costs.	Uncapacitated	Integer programming	Disaggregate	Decision variables under constraint that UAM has lower generalized cost.	Divide the study area into hexagons, then manually remove and combine some hexagons to reduce the number of candidates.	Solve the large-scale optimization problem (NP-hard) by adding additional constraints to reduce the feasible region.	Incorporate mode choice modeling problem as decision variables might be a deviation from realistic.

Table 1 continued from previous page

Paper	Objective	Vertiport's Capacity	Solution Approach	Travel Demand	Mode Choice	Vertiport Candidates	Innovative Points	Limitations
Willey and Salmon (2021)	Minimize travel time.	Uncapacitated	Heuristic algorithms	Aggregate	Probability of taking UAM is a function of travel time.	Already existing airports and helipads+ DBSCAN clustering.	Incorporate elements of subgraph isomorphism in the vertiport siting problem that allows for public transit operations.	Aggregated demand might be distorted. Only consider travel time as travel cost. The mode choice model is too simplistic.
Wang et al. (2022)	Maximize the efficiency and profitability of UAM operations.	Capacitated	Adaptive discretization	Aggregate	Multinomial logit model and distributional robust optimization	Consider factors such as demand hotspots, geographical distribution and operational feasibility.	Develop an integrated framework that captures the interdependencies between strategic vertiport planning, tactical operations, and passenger demand. Incorporate consideration of vertiport capacities, queuing network dynamics and demand functions in the model. Develop the adaptive discretization algorithm to solve the optimization problem.	Aggregate demand might be distorted. The model solves for the "end-state" network but fails for dynamic network expansions.
Rath and Chow (2022)	Maximize air taxi ridership/ maximize air taxi revenue.	Uncapacitated	Integer programming	Aggregate	Objective of the problem. Binary Logit Model (taxi and air taxi).	3 main airports+ 149 taxi zones from publicly available data.	Incorporate discrete choice model into the network optimization model and highlight complexity of modeling user-based behavior in optimization problem.	Use binary logit model as opposed to multinomial logit model, whose assumption is too simplistic. Aggregated demand might be distorted.
He et al. (2023)	Maximize the UAM ridership.	Uncapacitated	Hierarchical Optimization MEthod (HOME)	Aggregate	Same as Rath and Chow (2022)	Trip data is spatially aggregated into 4171 zones in which any zone can be a candidate.	Develop HOME algorithm to solve the large-scale network optimization problem.	Same as Rath and Chow (2022).

Table 1 continued from previous page

Paper	Objective	Vertiport's Capacity	Solution Approach	Travel Demand	Mode Choice	Vertiport Candidates	Innovative Points	Limitations
Boo et al. (2023)	Maximize accessibility of different sites to vertiports. Minimize land purchase costs. Minimize total aerial distance between vertiports.	Uncapacitated	ε-constraint methods	No consideration.	No consideration.	Existing airports.	Utilize ε-constraint methods to address the multi-objective optimization problem.	No consideration of real demand.
Brulin and Olhofer (2023)	Maximize UAM demand. Minimize number of vertiports.	Uncapacitated	Bi-network (GA+MATSim)	Disaggregate	MATSim scoring function.	Clustering-based methods with consideration of constraints of existing infrastructures.	Integrate MATSim agent-based simulation with network optimization.	The objectives of inner loop and outer loop are not consistent.
This study	Maximize the saved generalized travel costs.	Uncapacitated	Heuristic algorithms	Disaggregate	Multinomial discrete choice model.	K-means++ clustering	Formulate the vertiport siting as a two-stage stochastic optimization problem. Incorporate mode choice as a stochastic variable by simulating it with the discrete choice model. Develop 2 heuristic algorithms for solving the optimization problem.	Discussed in Section 8.

Table 2 Comparison of vertiports siting approaches.

Approach	Pros	Cons
Qualitative approaches		
Existing infrastructure	Low construction cost.	Limited locations and flexibility.
	Faster Implementation.	Limited consideration of UAM demand.
	Regulatory precedence.	
MCDA	Good integration with land-use patterns.	Expert opinion required, not generalizable.
	Stakeholder engagement.	Subjectivity in decision-making process.
	Consideration of multiple criteria.	
Quantitative approaches		
Clustering	Easy to perform.	No guarantee of optimal solution.
	Consideration of demand.	No incorporation with land-use patterns.
	Good generalizability.	Sensitivity in initialization.
Optimization	Guarantee of optimal solution.	Complexity in formulation and solving.
	Easy to perform.	No incorporation with land-use patterns.
	Consideration of demand.	
	Good generalizability.	

2.4. Research Gaps

By reviewing the existing studies regarding qualitative and quantitative vertiports siting approaches, the advantages and shortcomings of each method are summarized in Table 2. Among the various methodologies, optimization approaches have gained widespread acceptance due to their capability to yield optimal or nearly optimal solutions for predefined objectives while adhering to specified constraints. Their simplicity and generality make them highly practical. Nevertheless, in the context of selecting UAM vertiport locations, much of the existing research employing optimization methods has tended to overlook the stochastic nature of mode choice for disaggregated trips. Incorporating stochastic variables can indeed

significantly augment the complexity of optimization problems, but it also aligns them more closely with real-world scenarios. Furthermore, there has been a noticeable absence of emphasis on optimizing demand allocation, i.e., demand-vertiport matching. Previous research on demand allocation has primarily revolved around allocating demand points to fixed hub locations (e.g., the closest ones). To rectify these shortcomings, it becomes imperative to introduce the two-stage stochastic optimization frameworks.

2.5. Approaches for Solving Two-Stage Stochastic Optimization Problem

Two-stage stochastic optimization problems involve decision-making under uncertainty in two stages. In the first stage, decisions are made without knowing the realization of uncertain parameters, and in the second stage, decisions are made after the realization of uncertain parameters. The approach to solving a two-stage stochastic optimization problem typically involves formulating a mathematical model that incorporates the uncertainty and then using specialized solution techniques such as scenario-based or sample average approximation methods. It is a dynamic and evolving field, with ongoing research focusing on improving computational efficiency and applicability to real-world problems. This section provides a general introduction to the common and state-of-art solving approaches.

- Scenario-Based Approaches: These approaches involve creating a finite set of possible future scenarios to capture the uncertainty in the model. Each scenario is associated with a probability and specific outcomes, enabling the model to consider a range of possible future states (Rockafellar and Wets, 1991). This method is particularly useful in modeling complex uncertainties and is widely used in fields like finance and energy planning where future states are uncertain.

- Benders Decomposition: Benders Decomposition is a mathematical technique that decomposes a large-scale stochastic problem into smaller, more manageable sub-problems. It iteratively solves these sub-problems and communicates the solutions to a master problem (Geoffrion, 1972). This method is highly effective for problems where the first-stage and second-stage variables can be separated, significantly reducing computational complexity.

- Monte Carlo Sampling: Monte Carlo Sampling is used to approximate the probability distributions of uncertain parameters in stochastic models. It involves generating a large number of random samples to estimate the outcomes (Infanger, 1992). This approach is useful in scenarios where the probability distributions are complex or not analytically tractable, offering a practical way to incorporate randomness in the model. Here, Monte Carlo sampling refers to a set of algorithms for sampling from a probability distribution. For instance, Markov chain Monte Carlo (MCMC) was applied in Lu et al. (2024).

- Stochastic Dual Dynamic Programming (SDDP): SDDP is an algorithm designed for multi-stage stochastic problems, extending the principles of Benders decomposition (Pereira and Pinto, 1991). It is particularly adept at handling problems with a sequential decision-making structure. SDDP has found significant application in the energy sector, especially in hydrothermal scheduling, due to its efficiency in dealing with large-scale, multi-stage problems.

- Column-and-Constraint Generation: This method combines aspects of column generation (for efficiently handling a large number of scenarios) with constraint generation (for dealing with a large number of constraints in the master problem) (Zeng and Zhao, 2013). It is particularly useful for large-scale stochastic programming problems where traditional methods may struggle with the size and complexity of the problem.

- Robust Optimization: Robust Optimization focuses on finding solutions that are feasible and perform well across a range of different scenarios, rather than optimizing for a specific expected outcome. This approach is particularly useful when the probability distribution of uncertainties is unknown or unreliable (Rahimian and Mehrotra, 2019). It is a conservative approach that ensures the solutions are safeguarded against the worst-case scenarios, making it suitable for applications where reliability is crucial.

- Machine Learning Integration: Recent advancements integrate machine learning techniques to predict scenario probabilities, and outcomes, or to accelerate the solving process of stochastic programming models (Ning and You, 2019). This approach leverages the power of data-driven methods to enhance model accuracy and computational efficiency, particularly useful in dynamically changing environments where historical data can inform future decisions.

3. MCDA and Clustering Approaches for Vertiports Siting

As introduced in Section 2.2 and 2.3, MCDA and clustering are both commonly utilized vertiports siting approaches in numerous studies. Although this thesis proposes an optimization-based approach, it is still important to demonstrate the general processes and methodologies of MCDA and clustering in this chapter, as some procedures in this thesis draw inspiration from them.

3.1. Methodology of MCDA Approach

MCDA is a decision-making process that helps in evaluating and prioritizing different options based on multiple conflicting criteria. It is particularly useful in complex scenarios where decisions need to be made considering various factors, which may be quantitative or qualitative in nature (Triantaphyllou et al., 1998).

In MCDA, decision-makers first identify the criteria important for the decision at hand. These criteria represent different aspects or dimensions of the decision problem, such as cost, efficiency, effectiveness, and environmental impact. The relative importance of these criteria is then determined, often through weights that reflect their priority in the decision-making process. The next step involves evaluating each option or alternative against the identified criteria. This evaluation can be done through various methods, such as rating scales, cost-benefit analysis, or using specific decision-making tools and software. The final stage of MCDA involves aggregating the evaluations to rank the options. This can be done through various techniques like the AHP, Technique for Order of Preference by Similarity to Ideal Solution (TOPSIS), or the Simple Multi-Attribute Rating Technique (SMART) (Barron and Barrett, 1996; Lin et al., 2008). The end result is a ranking or score for each option, which guides the decision-maker in choosing the best alternative based on the given criteria and their respective weights.

In the context of UAM vertiports siting, the processes are generally consistent with the classical MCDA stages. Existing studies that utilized this method for vertiport siting have adopted AHP in the options ranking step. To better illustrate the application of MCDA to the vertiport siting problem, the detailed steps of the methodology are shown in Figure 4. The process is exemplified by the methodology described in the thesis of Fadhil (2018).
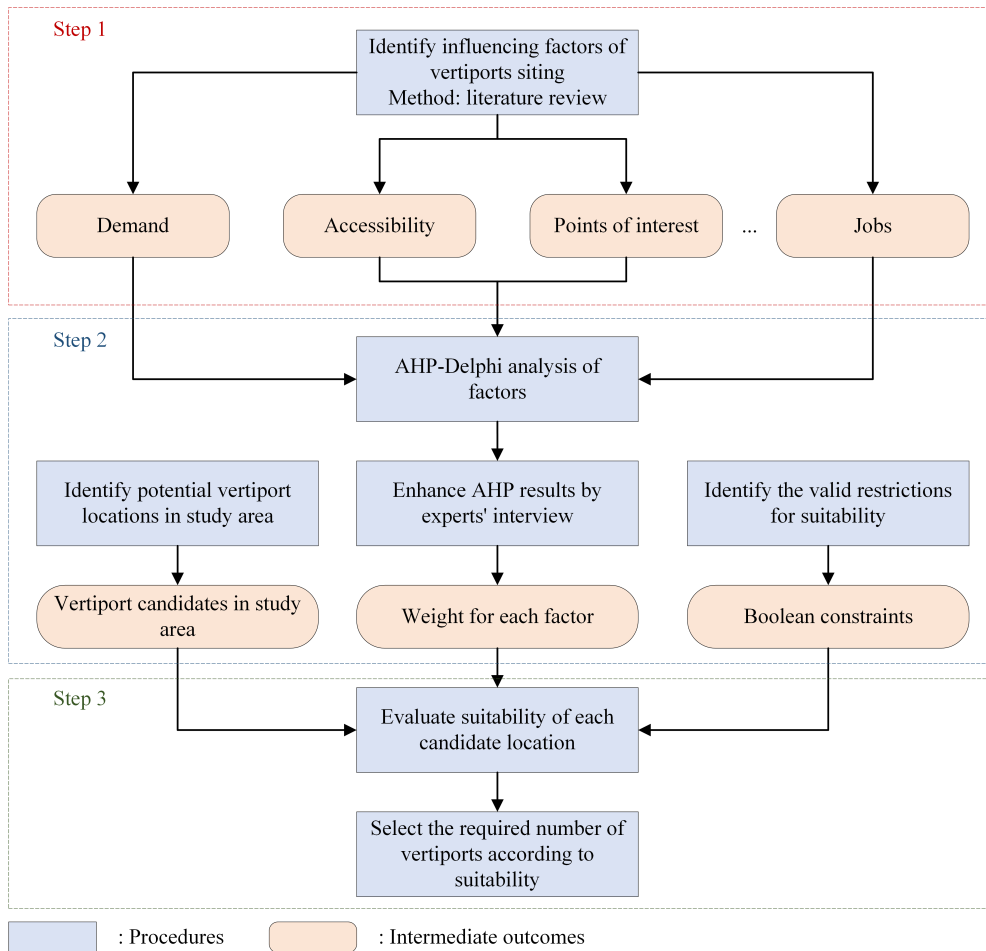
Figure 4 Framework of MCDA approach in vertiports siting.

3.2. Methodology of Clustering Approach

Clustering methods play a pivotal role in vertiport siting by grouping potential locations based on various criteria, such as proximity to demand centers, airspace safety, and infrastructural feasibility. As discussed in Section 2.3, almost all current studies that apply clustering to select UAM vertiport locations are demand-oriented. The consideration of demand in these studies varies, the most common is to use population distribution as the demand point, some others use trip data as the demand point, and so on. The clustering method is quite straightforward and simply involves clustering these demand points and then using the centroids of the clusters as potential vertiport locations. Unlike the MCDA and optimization methods, the clustering method does not require prior identification of candidate vertiport locations, which simplifies the research process. However, this is also a disadvantage because there is no way to artificially control that all these centroids are qualified to construct vertiports. Depending on the clustering algorithm, some can specify the number of clusters in advance to obtain a fixed number of vertiports, while others cannot and must iteratively adjust the parameters to obtain the specified number of vertiports.

As a matter of practice, after executing the clustering, scholars often need to evaluate the results, some of which are specific to the clustering itself (e.g., Davies–Bouldin index, Silhouette technique) and others from the perspective of the effectiveness of UAM operations (e.g., travel time, accessibility). The general methodology of the clustering approach in vertiports siting is demonstrated in Figure 5.
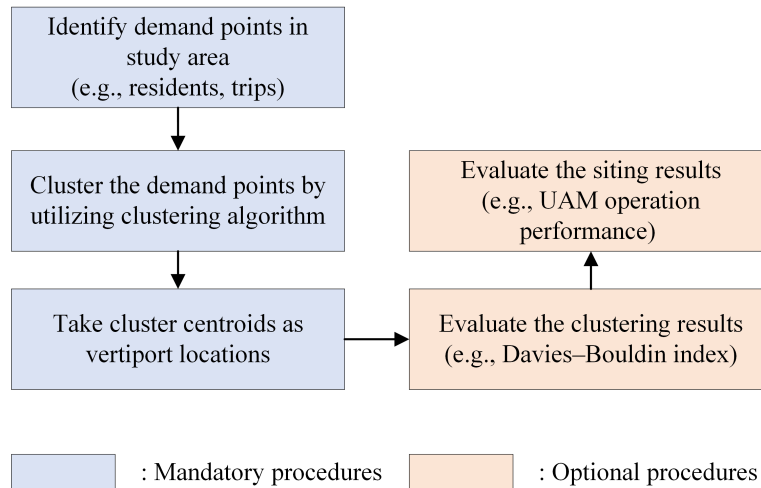
Figure 5 Framework of clustering approach in vertiports siting.

In summary, clustering methods in UAM vertiport siting are essential for systematically evaluating potential locations. They enable urban planners and UAM operators to make data-driven decisions, optimizing the placement of vertiports for maximum efficiency, safety, and urban compatibility. These methods consider a multitude of factors, from population density and urban layout to regulatory frameworks, ensuring that the development of UAM infrastructure is both practical and sustainable.

3.3. Integration with Optimization Approach

Although the vertiports siting method used in this thesis is optimization-based, the MCDA and clustering methods provide a lot of inspiration for the methodology of this thesis.

First, the initial step of the optimization-based vertiport siting method is to determine the vertiport candidates. Identifying vertiport candidates can be done by applying the clustering method, i.e., the centroids obtained from clustering are taken as the potential candidates. This method has been practiced by Holden and Goel (2016) with good results, and thus the same approach is used in this thesis. The detail of this part is explained in Section 6.2.

Second, as acknowledged in Section 2.4, it is often challenging for the optimization method to take into account multiple factors during the optimization process, which happens to be the strength of MCDA. Thus, this thesis will evaluate the results with the help of some of the factors involved in MCDA, namely demand coverage and accessibility enhancement after the

execution of the optimization algorithm. The detail of this part is explained in Sections 7.3 and 7.4.

4. Modeling Methodology

This study aims to utilize optimization methods for selecting vertiport locations among candidates to minimize the sum of generalized travel costs of all trips. As highlighted in Section 2.4, existing literature on UAM vertiport siting has encountered challenges in effectively capturing the stochastic nature of mode choice for disaggregated travel demand, which involves individual trip data. Most studies typically treated mode choice as either an optimized objective, a decision variable within the objective function, or employed mode choice modeling for aggregated travel demand. These approaches often struggle to precisely replicate the real choices made by travelers. To this end, we adopt a novel approach by treating individual
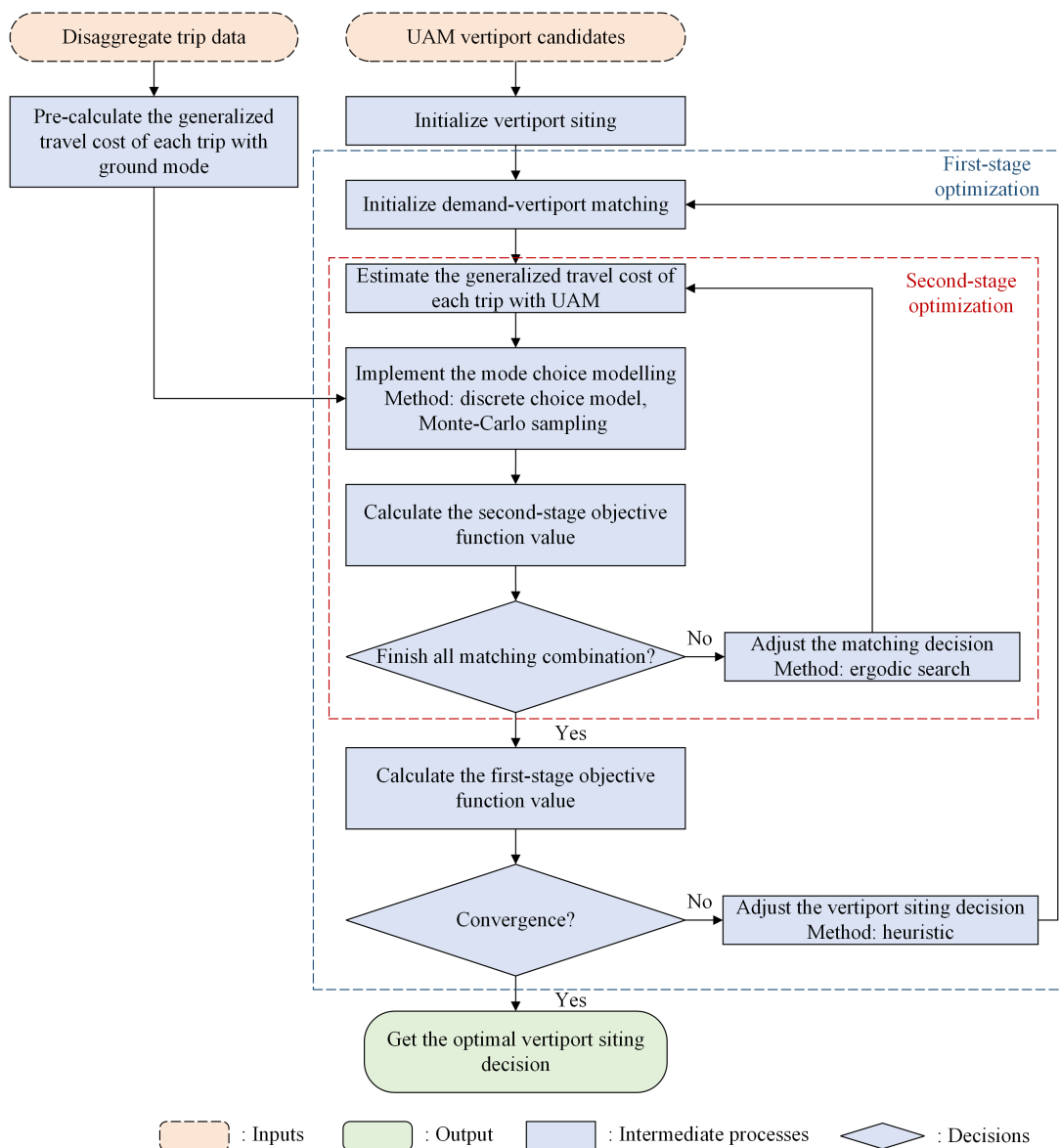
Figure 6 Two-stage stochastic optimization framework for UAM vertiport selection.

mode choice as a stochastic variable, and incorporate decision optimization at the demand-

vertiport matching stage. This unique formulation transforms the problem into a two-stage stochastic optimization. The general framework of this study is shown in Figure 6.

4.1. Assumptions

In the context of a defined study area, which includes a roster of potential UAM vertiport candidates denoted as M with the size of n, and an assemblage of disaggregated travel demand data represented by a list of trips, denoted as TR, this study endeavors to identify the optimal set of vertiports, designated as V and encompassing p elements selected from the set M. The primary objective of this endeavor is the minimization of the total generalized travel costs associated with the trips in list TR. To facilitate this formulation, we introduce the following assumptions:

Assumption 1 *UAM service is exclusively accessible for each trip when there exist vertiports situated within the catchment areas of both its origin and destination. The catchment area is defined as a neighboring circle with a fixed radius.*

Assumption 2 *The waiting times at UAM vertiports remain constant throughout this study. Any potential additional waiting times incurred by UAM travelers due to capacity limitations at vertiports or shortages of UAM vehicles (eVTOL aircraft) are not taken into account. In essence, the problem formulation adopted in this study pertains to an uncapacitated facility location problem.*

Assumption 3 *The UAM network is designed as a fully connected network, ensuring direct connectivity between all vertiports. Consequently, UAM trips do not involve any flight transfers at vertiports.*

4.2. Problem Formulation

Before delving into the formulation based on this context, it is worthwhile to review the general formulation of two-stage stochastic programming, as proposed by Birge and Louveaux (2011). In accordance with their exposition, the general two-stage stochastic programming framework is represented by Equation(4.1),

$$\min_{x \in X} \quad g(x) = f(x) + E_\xi[Q(x, \xi)] \tag{4.1}$$

where x represents the first-stage decision and the first component $f(x)$ constitutes an objective function solely dependent on the first-stage decision (deterministic component). The symbol ξ denotes a random parameter vector characterizing stochastic variables. The actual

realization of ξ remains unknown until an experiment is conducted. The experiment's outcome, denoted as ω, yields a specific realization of the random parameters, $\xi(\omega)$. The value $Q(x, \xi)$ represents the optimal solution of the second-stage problem once the first-stage decision x has been determined. It is defined by the following optimization problem:

$$Q(x, \xi) = \min_y \{q(y, \xi) \,|\, T(\xi)x + W(\xi)y = h(\xi)\} \tag{4.2}$$

where y represents the second-stage decision variable. Under this formulation, the first-stage decision variable is determined before the realization of the uncertain vector because its realization is unknown at the time of the first-stage decision. However, the objective function for the second-stage decision problem indeed calculates the expectation value. Once the first-stage decision is made, the second-stage decision problem can be solved based on specific realized parameter values at each time instance (Han and Lee, 2021).

Subsequently, Equation (4.1) and (4.2) need to be brought into the context of this vertiport siting problem. In the vertiport siting problem, the first-stage decision variable denoted as $\mathbf{x}$ is responsible for determining the locations of vertiports. Meanwhile, the second-stage decision variable $\mathbf{y}$ allocates the demand points. The overarching objective is to minimize the total generalized travel cost for all trips. They are bolded because they are actually both vectors (matrices), and are used to differentiate them from the x and y that describe the individual decisions. Apparently, the objective for optimizing, i.e., generalized travel cost, is a function intertwined with both stages of decision-making. Consequently, the objective function is reformulated as follows:

$$\min_{\mathbf{x} \in \mathbf{X}} \{g(\mathbf{x}) = E_{\boldsymbol{\xi}}[Q(\mathbf{x}, \boldsymbol{\xi})]\} \tag{4.3}$$

where $\mathbf{x}$ is the decision variable vector that signifies the selection of vertiports. The element x_i is a binary variable, taking a value of 1 if vertiport candidate i is chosen and 0 otherwise. In this study, the number of selected vertiports is fixed at p, and this constraint is represented by:

$$\sum_{i \in M} x_i = p \tag{4.4}$$

$$x_i \in \{0, 1\}, \forall i \in M \tag{4.5}$$

Once the selection of vertiports is determined, the second-stage objective function, which is the sum of the generalized travel costs for all trips, is given by Equation (4.6). This formulation draws inspiration from the generic p-median problem formulation by Farahani et al. (2013)

and the vertiport siting optimization formulation by Wu and Zhang (2021).

$$Q(\mathbf{x}, \boldsymbol{\xi}) = \min \sum_{tr \in TR} \Bigg\{ \sum_{g \in G} z_g^{tr}(t_g^{tr}\gamma^{tr} + c_g^{tr}) + (1 - \sum_{g \in G} z_g^{tr}) \sum_{k \in M} \sum_{m \in M, k \neq m} y_k^{tr} y_m^{tr} \Big[c_{km} + (t_{km} +$$

$$t_{tw} + t_{tp})\gamma^{tr} + \sum_{a \in A} z_a^{tr}(t_{ak}^{tr}\gamma^{tr} + c_{ak}^{tr}) + \sum_{e \in E} z_e^{tr}(t_{em}^{tr}\gamma^{tr} + c_{em}^{tr}) \Big] \Bigg\}$$

$$(4.6)$$

where,

$tr \in TR$: notation of trips.

$g \in G$: notation of ground-based transport modes.

z_g^{tr}: binary variable for ground-based transport mode. If trip tr is in mode g, $z_g^{tr} = 1$, otherwise, $z_g^{tr} = 0$.

t_g^{tr}: travel time of trip tr in mode g.

γ^{tr}: value of time (VOT) of trip tr, which is dependent on the income of the traveler.

c_g^{tr}: monetary travel cost of trip tr in mode g.

k, m, M: k, m are the index of origin and destination vertiports of a UAM trip, M is the set of all vertiports candidates.

y_k^{tr}, y_m^{tr}: binary decision variables for origin and destination vertiports allocation, $y_k^{tr} = 1$ if vertiport k is chosen as origin vertiport for trip tr, otherwise $y_k^{tr} = 0$. Similarly, $y_m^{tr} = 1$ if vertiport m is chosen as destination vertiport for trip tr, otherwise $y_m^{tr} = 0$.

c_{km}: monetary travel cost from vertiport k to m.

t_{km}: flying time from vertiport k to m.

t_{tw}: waiting time before on-boarding.

t_{tp}: processing time before onboarding and after landing.

$a \in A$: ground-based transport modes for access leg.

$e \in E$: ground-based transport modes for egress leg.

z_a^{tr}: binary variable for ground-based transport modes for access leg, $z_a^{tr} = 1$ if mode a is taken for accessing origin vertiport in trip tr, otherwise $z_a^{tr} = 0$.

z_e^{tr}: binary variable for ground-based transport modes for egress leg, $z_e^{tr} = 1$ if mode e is taken for egressing destination vertiport in trip tr, otherwise $z_e^{tr} = 0$.

t_{ak}^{tr}: travel time of access leg to origin vertiport k in mode a of trip tr.

c_{ak}^{tr}: monetary travel cost of access leg to origin vertiport k in mode a of trip tr.

t_{em}^{tr}: travel time of egress leg from destination vertiport m in mode e of trip tr.

c_{em}^{tr}: monetary travel cost of egress leg from destination vertiport m in mode e of trip tr.

As illustrated in Equation (4.6), the generalized travel cost for each trip tr comprises two components based on the mode choice. The first component represents the generalized cost when taking ground-based transport modes, while the second component represents the generalized cost when using UAM. The latter includes the generalized costs associated with the access, flight, and egress legs. In this two-stage optimization problem, the variables $\mathbf{x}$, $\mathbf{y}_k$, and $\mathbf{y}_m$ are vectors (or matrices) of decision variables in the first and second stages.

They respectively denote the choices for vertiport selection, origin-vertiport allocation, and destination-vertiport allocation. To identify the feasible region of these decision variables as well as the possible realizations of stochastic variables, the constraints will be discussed in the following part.

In a single realization scenario for stochastic variables, for each trip denoted as tr, the primary transport mode can be either pure ground-based or UAM-based. To account for all possible experimental outcomes related to mode choice for a trip, the following constraints are formulated:

$$\sum_{g \in G} z_g^{tr} + \sum_{a \in A} z_a^{tr} \sum_{e \in E} z_e^{tr} = 1 \qquad \forall tr \in TR \tag{4.7}$$

$$\sum_{a \in A} z_a^{tr} = \sum_{e \in E} z_e^{tr} \qquad \forall tr \in TR \tag{4.8}$$

$$z_g^{tr}, z_a^{tr}, z_e^{tr} \in \{0,1\} \qquad \forall g \in G, a \in A, e \in E, tr \in TR \tag{4.9}$$

Furthermore, locations denoted as k and m are only eligible to be selected as the origin and destination vertiports, respectively, if vertiports have been constructed at candidates k and m. This constraint can be formulated as follows:

$$y_k^{tr} \le x_k, y_m^{tr} \le x_m \qquad \forall tr \in TR, k \in M, m \in M, m \ne k \tag{4.10}$$

$$y_k^{tr} \in \{0,1\}, y_m^{tr} \in \{0,1\} \qquad \forall tr \in TR, k \in M, m \in M, m \ne k \tag{4.11}$$

The demand allocation strategy in this study is single allocation, i.e., a demand point will only end up being assigned to one vertiport in the second stage of decision-making. This constraint can be expressed as follows:

$$\sum_{k \in M} y_k^{tr} = 1, \sum_{m \in M} y_m^{tr} = 1 \qquad \forall tr \in TR, k \in M, m \in M, m \ne k \tag{4.12}$$

So far, the formulation of this two-stage stochastic programming is completed, encompassing the objective function in Equations(4.3) and (4.6) along with the constraints detailed in Equations(4.4)-(4.5) and (4.7)-(4.12).

The constraints introduced above establish the feasible regions for the decision variables as well as the random variables, providing a comprehensive framework for solving the problem. The formulation given by Equations(4.3) and (4.6) is denoted as FM1. Furthermore, considering that the time, expenses, and generalized costs associated with ground-based transport modes are known and constant for each trip, it becomes apparent that the primary objective of minimizing the generalized cost for all trips in FM1 is essentially equivalent to maximizing the savings in generalized travel costs facilitated by UAM services, as proposed by Wu and Zhang (2021). The new formulation is denoted as FM2. In contrast to FM1, FM2 offers a

more intuitive perspective on the genuine macroeconomic advantages introduced by UAM services, specifically, the reduction in overall generalized travel costs. The mathematical formulation is illustrated as follows:

$$\max_{\mathbf{x} \in \mathbf{X}} \quad g(\mathbf{x}) = E_{\boldsymbol{\xi}}[Q(\mathbf{x}, \boldsymbol{\xi})] \tag{4.13}$$

$$Q(\mathbf{x}, \boldsymbol{\xi}) = \max \sum_{tr \in TR} \left\{ h^{tr} - \sum_{g \in G} z_g^{tr}(t_g^{tr}\gamma^{tr} + c_g^{tr}) - (1 - \sum_{g \in G} z_g^{tr}) \sum_{k \in M} \sum_{m \in M, k \neq m} y_k^{tr} y_m^{tr} \Big[c_{km} + \right.$$
$$\left. (t_{km} + t_{tw} + t_{tp})\gamma^{tr} + \sum_{a \in A} z_a^{tr}(t_{ak}^{tr}.\gamma^{tr} + c_{ak}^{tr}) + \sum_{e \in E} z_e^{tr}(t_{em}^{tr}\gamma^{tr} + c_{em}^{tr}) \Big] \right\}$$
$$\tag{4.14}$$

where,

h^{tr}: the generalized travel cost of trip tr taking ground-based transport mode.

$tr \in TR$: notation of trips.

$g \in G$: notation of ground-based transport modes.

z_g^{tr}: binary variable for ground-based transport mode. If trip tr is in mode g, $z_g^{tr} = 1$, otherwise, $z_g^{tr} = 0$.

t_g^{tr}: travel time of trip tr in mode g.

γ^{tr}: VOT of trip tr, which is dependent on the income of the traveler.

c_g^{tr}: monetary travel cost of trip tr in mode g.

k, m, M: k, m are the index of origin and destination vertiports of a UAM trip, M is the set of all vertiports candidates.

y_k^{tr}, y_m^{tr}: binary decision variables for origin and destination vertiports allocation, $y_k^{tr} = 1$ if vertiport k is chosen as origin vertiport for trip tr, otherwise $y_k^{tr} = 0$. Similarly, $y_m^{tr} = 1$ if vertiport m is chosen as destination vertiport for trip tr, otherwise $y_m^{tr} = 0$.

c_{km}: monetary travel cost from vertiport k to m.

t_{km}: flying time from vertiport k to m.

t_{tw}: waiting time before on-boarding.

t_{tp}: processing time before onboarding and after landing.

$a \in A$: ground-based transport modes for access leg.

$e \in E$: ground-based transport modes for egress leg.

z_a^{tr}: binary variable for ground-based transport modes for access leg, $z_a^{tr} = 1$ if mode a is taken for accessing origin vertiport in trip tr, otherwise $z_a^{tr} = 0$.

z_e^{tr}: binary variable for ground-based transport modes for egress leg, $z_e^{tr} = 1$ if mode e is taken for egressing destination vertiport in trip tr, otherwise $z_e^{tr} = 0$.

t_{ak}^{tr}: travel time of access leg to origin vertiport k in mode a of trip tr.

c_{ak}^{tr}: monetary travel cost of access leg to origin vertiport k in mode a of trip tr.

t_{em}^{tr}: travel time of egress leg from destination vertiport m in mode e of trip tr.

c_{em}^{tr}: monetary travel cost of egress leg from destination vertiport m in mode e of trip tr.

4.3. Mode Choice Modeling

As explained in Section 4.2, it is important to note that the stochastic parameter vector, which pertains to the mode choice variables for each trip in this context, can only be realized after both stages of decision-making are completed. To elaborate, once the vertiport locations are fixed, the OD for a trip are allocated to a specific vertiport pair without prior knowledge of the chosen mode. Subsequently, based on the current allocation decision, various travel-related variables, such as travel time, cost, and distance can be estimated for each potential mode choice. The discrete choice model is a common approach for predicting future choices based on observed preferences. Particularly in the field of transportation, it is used in many studies to understand the mode choice preference of travelers (Straubinger et al., 2021). Thus, in the subsequent step, the utility associated with each mode is estimated using a discrete choice model. This model takes into account not only mode-specific attributes (e.g., travel cost, in-vehicle time, and waiting time), but also travel behavior attributes (including car ownership, trip purpose, and previous mode choice), and sociodemographic attributes (e.g., age, income, gender, and occupation). The probability of selecting each mode for all travelers can be calculated as follows:

$$p(z_g^{tr} = 1|\mathbf{x}, \mathbf{y}, tr) = D(\mathbf{x}, \mathbf{y}, tr) \qquad \forall g \in G, tr \in TR \qquad (4.15)$$

$$p(z_a^{tr} = 1|\mathbf{x}, \mathbf{y}, tr) = D(\mathbf{x}, \mathbf{y}, tr) \qquad \forall a \in A, tr \in TR \qquad (4.16)$$

$$p(z_e^{tr} = 1|\mathbf{x}, \mathbf{y}, tr) = D(\mathbf{x}, \mathbf{y}, tr) \qquad \forall e \in E, tr \in TR \qquad (4.17)$$

where D refers to the function of the discrete choice model.

Monte Carlo sampling is then applied to determine the mode choice outcomes based on the estimated probabilities. Each sample from Monte Carlo is referred to as a scenario, and it can be represented as follows:

$$z_g^{tr}, z_a^{tr}, z_e^{tr} = MC[p(z_g^{tr} = 1), p(z_a^{tr} = 1), p(z_e^{tr} = 1)] \qquad (4.18)$$

where MC denotes the Monte Carlo sampling process. It is important to note that the outcomes of Monte Carlo sampling must adhere to the constraints outlined in Equation (4.7)-(4.9).

In the field of large-scale stochastic programming, a significant number of scenarios is often required to encompass various potential realizations of stochastic variables. In this study, due to the independence of trips from each other, it is feasible to sample and solve for each trip separately. That means, for each trip, a list of mode choice scenarios will be drawn out by Monte Carlo sampling, the generalized travel cost of this trip will then be calculated as the expected value across all scenarios.

Up to this point, the mode choice modeling has been fully developed. It is important to

highlight that in this problem, the stochastic variable z, representing mode choice, is only realized after both stages of decision-making (vertiport siting and demand allocation) have been completed. In other words, the stochastic variable in this problem is not independent; rather, it depends on the outcomes of the decisions. This type of problem is referred to as an endogenous uncertainty problem, as classified by Goel and Grossmann (2006), distinguishing it from classical two-stage stochastic programming, which typically deals with exogenous uncertainty problems. Particularly, the uncertainty in this problem depends on the decisions made in both stages. To the best of the authors' knowledge, there is no existing literature or research on decomposition strategies specifically tailored to address this type of problem.

5. Solution Approaches

5.1. Demand Allocation Optimization
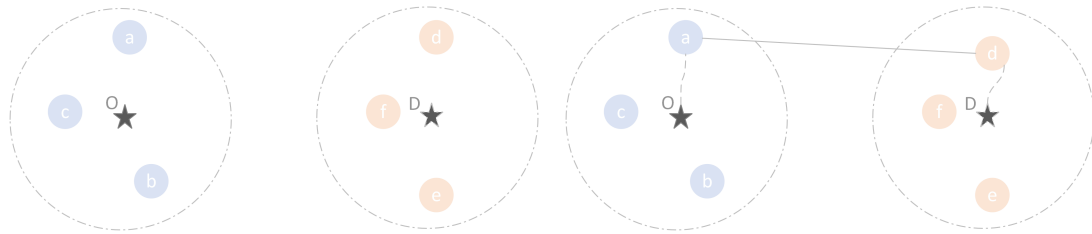
(a) Identify all available vertiports located within the catchment area of origin and destination.

(b) With a given allocation scheme, execute mode choice modeling, estimate the expected value of saved generalized travel cost across all mode choice scenarios.
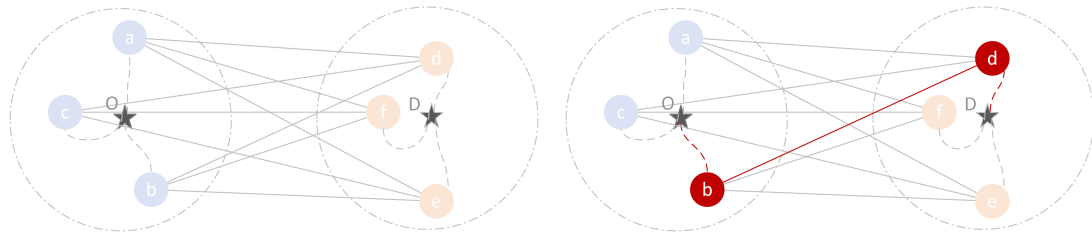
(c) Repeat the process for all possible allocation combinations.

(d) The optimal decision of second-stage for this trip is the allocation scheme with the highest expected saved generalized travel cost.

★ : origin and destination point of a trip

—— : flight route between vertiports

– – – : access/ egress leg to/ from vertiports

◯ : catchment area of demand points

a : vertiports within search radius of a trip's origin

d : vertiports within search radius of a trip's destination

d : optimal vertiports matched to trip's origin and destination

Figure 7 Demand-vertiport allocation processes.

To simplify the second stage of optimization, specifically the demand-vertiport matching process, we employed a strategy of defining catchment areas to limit the feasible region for decision variables. Practically, travelers are unlikely to select vertiports significantly distant from their trip's origin and destination for UAM services, as this could result in substantial detours. Therefore, we assume that trip origins and destinations can only be allocated to vertiports within their respective catchment areas, meaning a vertiport serves only nearby demand points. For instance, the matching process for a single trip is illustrated in Figure 7. Given that trips are independent, an ergodic search is suitable for demand allocation optimization. The algorithm iterates through all vertiport pairs within a trip's catchment area. For each allocation scheme, the mode choice modeling, as described in Section 4.3, is applied, and the expected savings in generalized travel cost for all scenarios are calculated. Ultimately, the trip's origin and destination are assigned to the vertiport pair offering the highest

expected savings in generalized travel cost.

5.2. Vertiports Siting Optimization

This section outlines the first-stage optimization process, focusing on vertiport location selection, following our discussion on stochastic variable realization (mode choice modeling) and second-stage optimization (demand-vertiport matching). As identified by Alumur and Kara (2008) and supported by various studies (Wu and Zhang, 2021; Willey and Salmon, 2021; He et al., 2023), the HLP is categorized as non-deterministic polynomial (NP)-hard, meaning it is not solvable within polynomial time. To address this, we implemented five heuristic optimization methods: Greedy Forwards (GRDF), Greedy Forwards Update (GRDF-U), Greedy Backwards (GRDB), Genetic Algorithm (GA), and Simulated Annealing (SA), to determine the most effective vertiport siting solution. Detailed descriptions of these algorithms' application to our specific problem will be presented in the following subsections.

5.2.1. Greedy Forwards (GRDF) Algorithm
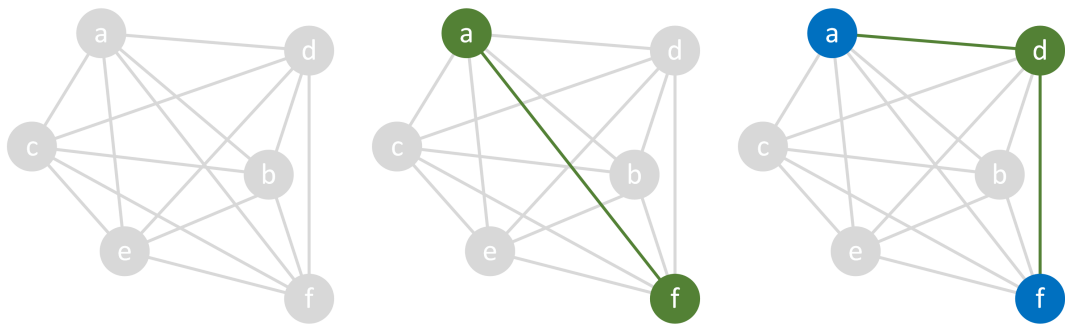
(a) Calculate the score of each vertiports pair route.

(b) Start from the vertiports pair with the highest score.

(c) Select the next vertiport (green) with the highest sum of scores of routes (green) it forms with all already selected vertiports (blue).
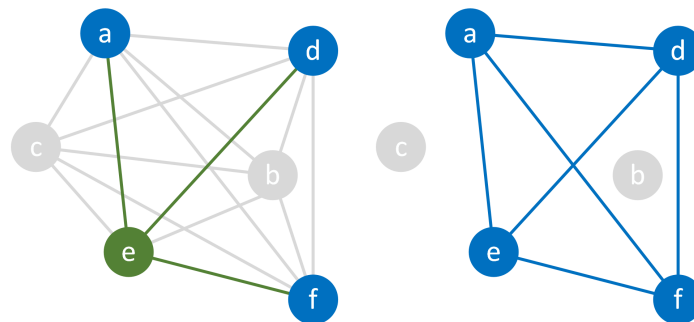
(d) Repeat the selection process to find the next vertiport.

(e) Algorithm stops when required number of vertiports are selected.

a : Vertiports that are not selected   a : Vertiports that are being selected in the current step   a : Vertiports that are already selected

Figure 8 GRDF algorithm processes.

Algorithm 1 GRDF Selection Algorithm

1: Input: M, TR, p; Output: V
2: $V \leftarrow \varnothing, R \leftarrow M$
3: $MaxRouteScore \leftarrow -\infty$
4: **for** each k in V **do**
5:    **for** each m in V, $m \neq k$ **do**
6:       Calculate route score $S(k, m)$
7:       **if** $S(k, m) > MaxRouteScore$ **then**
8:          $MaxRouteScore \leftarrow S(k, m)$
9:          $V \leftarrow \{k, m\}$
10:       **end if**
11:    **end for**
12: **end for**
13: $R \leftarrow R \setminus V$
14: **while** $|V| < p$ **do**
15:    $MaxSumScore \leftarrow -\infty$
16:    **for** each r in R **do**
17:       **if** $\sum_{v \in V} S(r, v) > MaxSumScore$ **then**
18:          $MaxSumScore \leftarrow \sum_{v \in V} S(r, v)$
19:          $currentVertiport \leftarrow r$
20:       **end if**
21:    **end for**
22:    $V \leftarrow V \cup \{r\}, R \leftarrow R \setminus \{r\}$
23: **end while**
24: Return V

The design and implementation of the GRDF algorithm in this problem draws inspiration from Willey and Salmon (2021). Before delving into the specifics of how GRDF operates, it's essential to clarify a fundamental concept: the scores of UAM routes. Imagine a scenario where only two UAM vertiports, labeled k and m, are chosen from all candidates, creating the simplest UAM network or route. The score of this route, $S(k, m)$, is defined by the expected savings in generalized travel costs achieved after the second-stage optimization. Understanding route scores is key to comprehending the GRDF process. Initially, the score of each pair of vertiports among all candidates is calculated. The first two vertiports selected are those forming the pair with the highest score. In each subsequent iteration, the process entails computing the sum of scores for each unselected vertiport when combined with all the already selected vertiports to form routes. The vertiport that yields the maximum sum is selected in that particular iteration. This process continues until the target number of vertiports is reached. A key feature of the GRDF algorithm is its unidirectional nature, meaning once a vertiport is selected, it will not be reconsidered for removal. An illustrative diagram showing the selection of 4 vertiports from 6 candidates is presented in Figure 8. Besides, the pseudo-code for this algorithm is also provided in Algorithm 1 for reference.

(a) Calculate the score of each vertiports pair route.

(b) Start from the vertiports pair with the highest score.

(c) Select the next vertiport (green) with the highest score of the network (green) it forms with all already selected vertiports (blue).
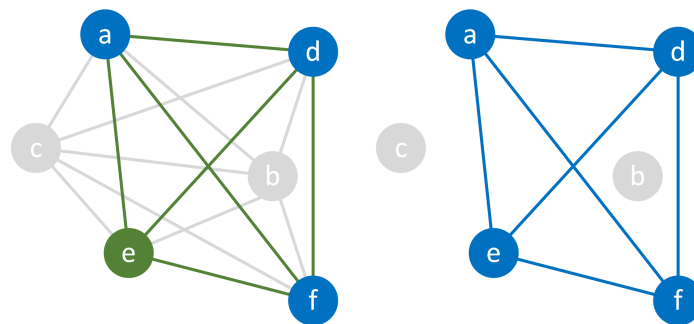
(d) Repeat the selection process to find the next vertiport.

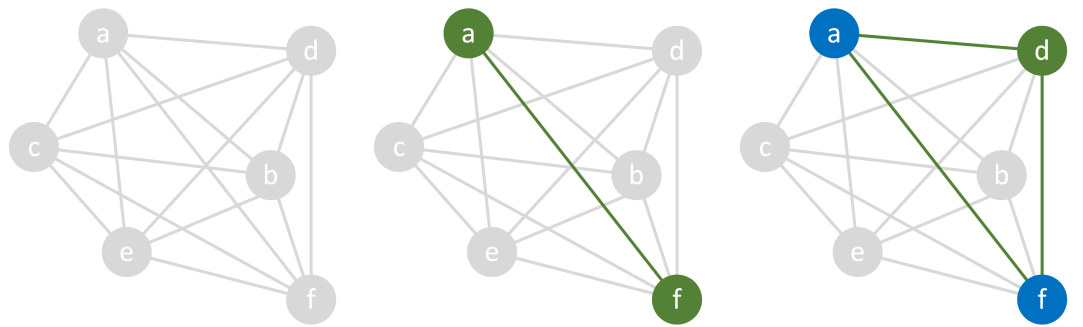(e) Algorithm stops when required number of vertiports are selected.

Figure 9 GRDF-U algorithm processes.

5.2.2. Greedy Forwards Update (GRDF-U) Algorithm

The fundamental approach of GRDF-U closely mirrors that of the GRDF algorithm, beginning with a pair of vertiports and incrementally adding new ones. However, key differences between GRDF-U and GRDF emerge upon a deeper exploration of the "score" concept.

As detailed in Section 5.2.1, a UAM route's score reflects the maximum saved generalized travel costs (from the second-stage objective function) achievable with just those two vertiports. This concept extends to a larger UAM network comprising multiple vertiports (e.g., k, l, m, n), where the network's score, $S(k, l, m, n)$, represents the maximum saved costs it can generate. The divergence between GRDF-U and GRDF is evident in their selection criteria during iterations. In GRDF-U, the decision to include a new vertiport is based not on the sum of scores for potential routes formed with existing vertiports but on the score of the entire UAM network formed by adding the new vertiport to the pre-selected ones. The chosen vertiport is the one that maximizes the network's overall score. Figure 9 visually demonstrates the GRDF-U process, with legends and notations consistent with those in Figure 8. Similarly, the pseudo-code of this algorithm is also shown below in Algorithm 2.

Algorithm 2 GRDF-U Selection Algorithm

1: Input: M, TR, p
2: $V \leftarrow \varnothing, R \leftarrow M$
3: $MaxRouteScore \leftarrow -\infty$
4: **for** each k in V **do**
5:     **for** each m in $V, m \neq k$ **do**
6:         Calculate route score $S(k, m)$
7:         **if** $S(k, m) > MaxRouteScore$ **then**
8:             $MaxRouteScore \leftarrow S(k, m)$
9:             $V \leftarrow \{k, m\}$
10:         **end if**
11:     **end for**
12: **end for**
13: $R \leftarrow R \setminus V$
14: **while** $|V| < p$ **do**
15:     $MaxNetworkScore \leftarrow -\infty$
16:     **for** each r in R **do**
17:         **if** $S(V \cup \{r\}) > MaxNetworkScore$ **then**
18:             $MaxNetworkScore \leftarrow S(V \cup \{r\})$
19:             $currentVertiport \leftarrow r$
20:         **end if**
21:     **end for**
22:     $V \leftarrow V \cup \{r\}, R \leftarrow R \setminus \{r\}$
23: **end while**
24: Return V

5.2.3. Greedy Backwards (GRDB) Algorithm

Another variant of the greedy algorithm is the GRDB algorithm. As indicated by its name, the GRDB algorithm operates under the premise that initially, all vertiport candidates are selected and each is assigned an initial weight of zero, symbolized as ω.

Algorithm 3 GRDB Selection Algorithm

Input: M, TR, p; Output: V
$V \leftarrow M$
for each v in V **do**
    $\omega_v = 0$
end for
for each tr in TR **do**
    Execute demand allocation Optimization, get the matched vertiports pair o and d
    Calculate saved generalized travel cost Q_{tr}
    $\omega_o \leftarrow \omega_o + Q_{tr}/2, \omega_d \leftarrow \omega_d + Q_{tr}/2$
end for
Sort the V in descending order by ω
$V \leftarrow$ first p elements of V
Return V

In our application, this approach diverges from conventional backward algorithms, as vertiports are not eliminated in each iteration. Rather, iterations in GRDB are characterized by

modeling for a single trip, not by the addition or subtraction of vertiports. In every iteration, demand-vertiport matching and mode choice modeling are performed for a specific trip, as detailed in sections 4.3 and 5.1. The origin and destination of the trip are assigned to the optimal pair of vertiports, and the expected value of saved generalized travel cost, Q, is calculated. This value, Q, is then evenly distributed among the weights of the two allocated vertiports. Upon completing iterations for all trips, vertiports are ranked based on their accumulated weights, and the top p vertiports with the highest weights are selected. Figure 10 visually depicts this process for clarity. The legend and notations used are in alignment with those in Figures 7, 8, and 9. Additionally, for a comprehensive understanding, the pseudocode for the GRDB algorithm is provided in Algorithm 3, highlighting their deviations from classical greedy algorithms.

(a) Assume all vertiport candidates are selected. All of them are assigned an initial weight ω of 0.

(b) For a trip, identify all available vertiports located within the catchment area of origin and destination.

(c) Execute demand allocation and mode choice modeling of the trip, find the optimal allocation scheme and the expected saved generalized travel cost Q. Distribute Q to weights of the vertiport pairs.

(d) After iterating over all trips, select the required number of vertiports with the highest weights.

Figure 10 GRDB algorithm processes.

5.2.4. Genetic Algorithm (GA)

The GA employed in this research is a search meta-heuristic, deriving its principles from Charles Darwin's theory of natural evolution. This algorithm emulates natural selection, where the most suitable individuals are chosen for reproduction to generate the subsequent generation's offspring.
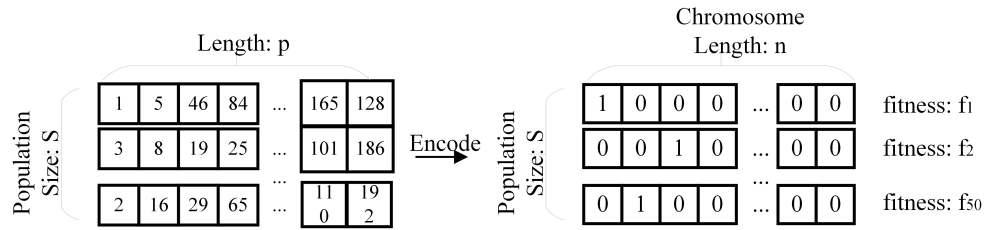
(a) Encode of Chromosomes of Generation 0
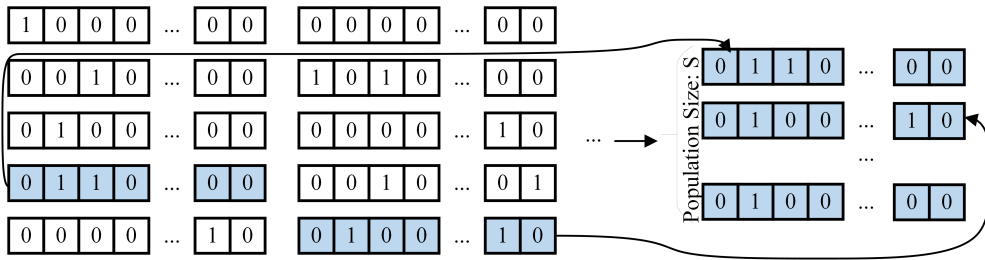
(b) Selection
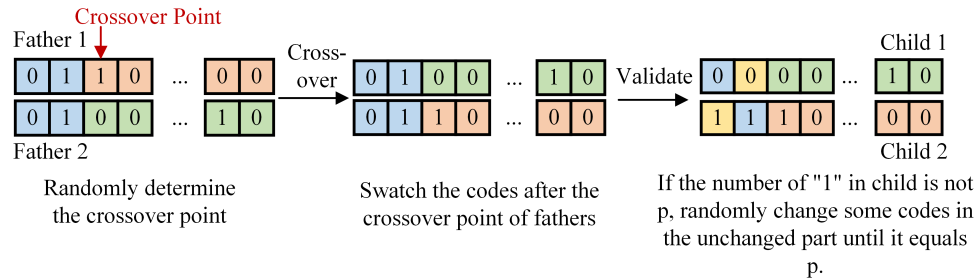
(c) Crossover and Validation
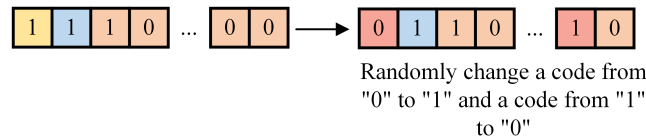
(d) Mutation
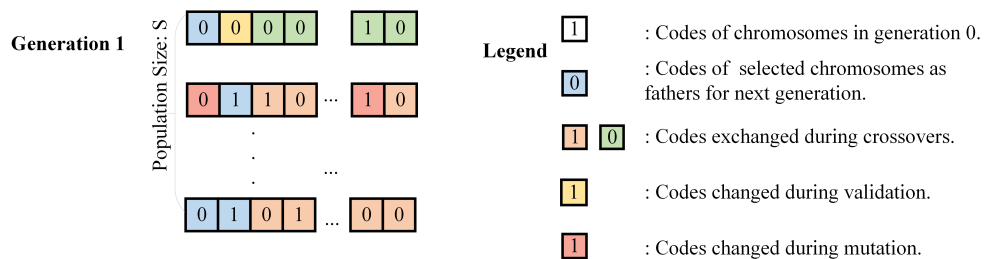
(e) Generation 1 and Legend

Figure 11 Evolution processes in GA.

In our application, a set containing selected vertiport IDs, with a size of p, is encoded as a binary "chromosome" with a length of n. A population comprises q such chromosomes, thereby defining the population size as q. The initial population is formed by encoding q

randomly generated solutions into chromosomes. Each iteration of the evolution process involves calculating the fitness value for every chromosome, based on the saved generalized travel costs in this context. A selection strategy is employed to choose q parent chromosomes for the next generation. These parents undergo crossover to produce offspring chromosomes. Given the constraints of this study, each binary-encoded chromosome must maintain exactly p "1" codes. Post-crossover, adjustments in the non-crossover segments of the chromosomes ensure that offspring chromosomes also contain exactly p "1" codes, a step termed "validatio". Additionally, the mutation occurs with a certain probability in the offspring chromosomes, promoting genetic diversity and averting local optima stagnation. This mutation involves swapping a selected "0" and "1" code in the chromosome. The algorithm iterates until a predefined termination condition, such as reaching the maximum number of generations or consecutive generations without improvement, is met. These conditions are known as "maximum generation" and "maximum generation without improvement", respectively. Figure 11 illustrates the algorithm's workflow in detail. Due to the classical nature of this algorithm and minor modifications in our study, a pseudo-code is not provided.

5.2.5. Simulated Annealing (SA) Algorithm

Simulated Annealing (SA) is a probabilistic optimization algorithm used for approximating solutions to complex optimization problems, particularly when exact solutions are computationally infeasible. This algorithm, inspired by the metallurgical process of annealing, begins with an initial solution and progressively explores adjacent solutions through random modifications. If a neighboring solution is superior, it is always accepted; however, the SA algorithm can also accept inferior solutions based on a probability influenced by a "temperature" parameter. Higher initial temperatures allow for more frequent acceptance of less optimal solutions, aiding in avoiding local optima. As the temperature gradually cools down, the likelihood of accepting worse solutions diminishes, steering the algorithm towards an improved solution.

Within this study's framework, a solution is defined as an array of selected vertiport IDs. The search for neighboring solutions involves randomly substituting one ID with an unselected candidate's ID. The effectiveness of each solution is gauged by its "energy", calculated from the saved generalized travel cost. The energy function plays a crucial role in Simulated Annealing, as it provides a quantitative measure of a solution's quality. Solutions with higher energy are considered more optimal. This energy-based evaluation allows the algorithm to quantify and compare different configurations of vertiport IDs effectively, ensuring a comprehensive search of the solution space.

Similar to the GA, SA continues until it either reaches the maximum number of iterations or fails to enhance the optimal solution over a series of consecutive iterations. This termination condition ensures that the algorithm does not run indefinitely and stops when it is no longer yielding significant improvements. The gradual cooling schedule of the SA algorithm is pivotal to its performance, as it balances exploration and exploitation of the solution space. Initially,

the algorithm explores a wide range of solutions, including those that are not immediately promising. As the temperature decreases, the focus shifts to exploiting the more promising regions of the solution space, fine-tuning the solutions to achieve near-optimal results.

The flowchart demonstrating the processes of SA is shown in Figure 12. Given the well-established nature of the Simulated Annealing algorithm and its wide recognition in the field of optimization, providing a pseudo-code for SA is deemed unnecessary. This decision is based on the assumption that the core concepts and operational mechanics of SA are sufficiently covered in standard computational optimization literature and are familiar to individuals with a background in this area.
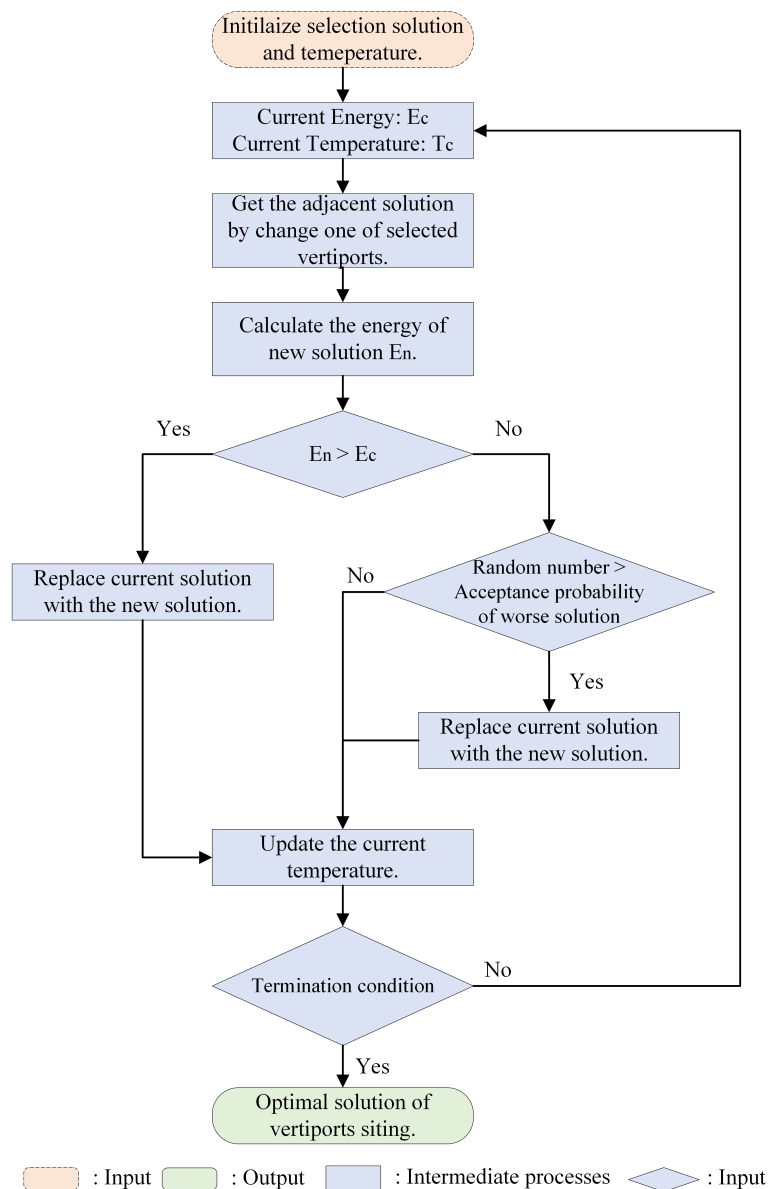
Figure 12 Processes of SA algorithm.

6. Experiment Design

6.1. Data Description

The study area of the study is Munich Metropolitan Area (MUC), Germany which has an approximate population of 4.5 million and encompasses 444 municipalities. The core cities include Munich, Augsburg, Ingolstadt, Landshut, and Rosenheim. The geographical scope of the study area coincides with that of previous UAM studies (Ploetner et al., 2020; Rothfeld, 2021; Rothfeld et al., 2021; Arellano, 2020; Fadhil, 2018; Guo et al., 2024). The trip data used in this optimization problem is generated and calibrated by Simple Integrated Land Use Orchestrator (SILO) and Microsimulation Transport Orchestrator (MITO), developed by Moeckel et al. (2020) and integrated the advantages of traditional trip-based and activity-based model. The trip data generated for the study area represent the scenario of an exemplary workday and encompass about 12.6 Million trips made by more than 4 million synthetic population. According to the conclusions by Guo et al. (2024), UAM only begins to show an upper hand in terms of time savings relative to ground transport over long-distance trips of 25 km or more, which is also largely consistent with the conclusion by Rothfeld et al. (2021) and Wu and Zhang (2021). Consequently, to reduce computational complexity, motorized trips exceeding 25 kilometers are selected for analysis. This subset of the dataset comprises a total of 454,513 trips. A visualization depicting the origin and destination points within the study area is presented in Figure 13.
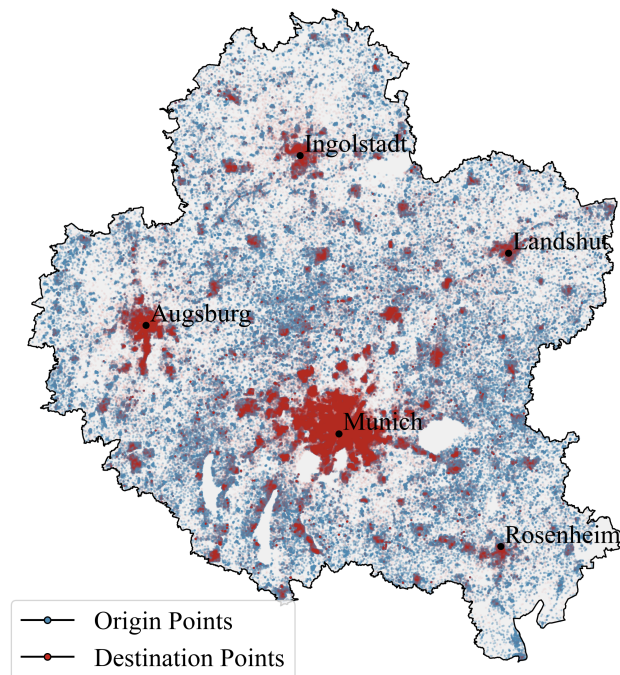
Figure 13 Demand points of MUC.

6.2. Vertiport Candidates Identification

In this study, vertiport candidates in the study area are identified by using K-means++ clustering, with the origins and destinations of long-distance trips mentioned above as data points, since Guo et al. (2024) suggested that the K-means++ clustering yields the best performance in both travel time savings and accessibility improvements in the context of vertiport siting. The number of vertiport candidates is determined as 200, which is already largely greater than it is in the densest UAM network (i.e., 130 vertiports) by Ploetner et al. (2020) and can cover more than 90% of the travel demands. The distribution of UAM vertiport candidates and covered demand points are shown in Figure 14(a) and 14(b), respectively. In order to have a clear understanding of the demand coverage level, when visualizing, the entire research area has been divided into 618 zones based on postal codes. The demand coverage rate within each zone will be presented using different colors on the spectrum. This zonal system is also applicable in the subsequent accessibility improvement assessment discussed in the following sections.

(a) Vertiport candidates.   (b) Vertiport candidates demand coverage rate.
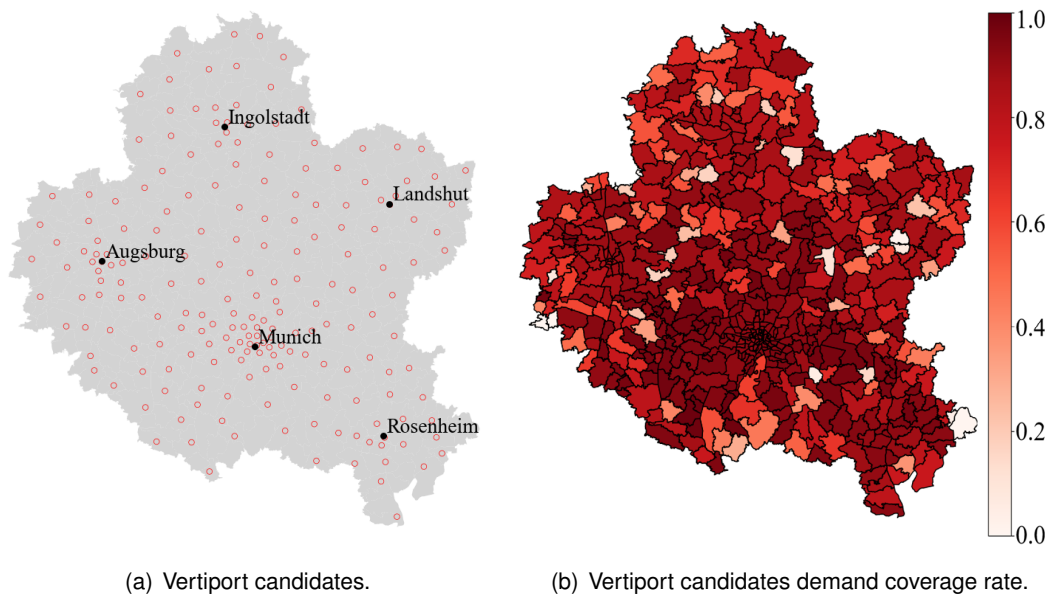
Figure 14 Vertiport candidates and demand coverage rate of vertiport candidates.

6.3. Data Preprocessing
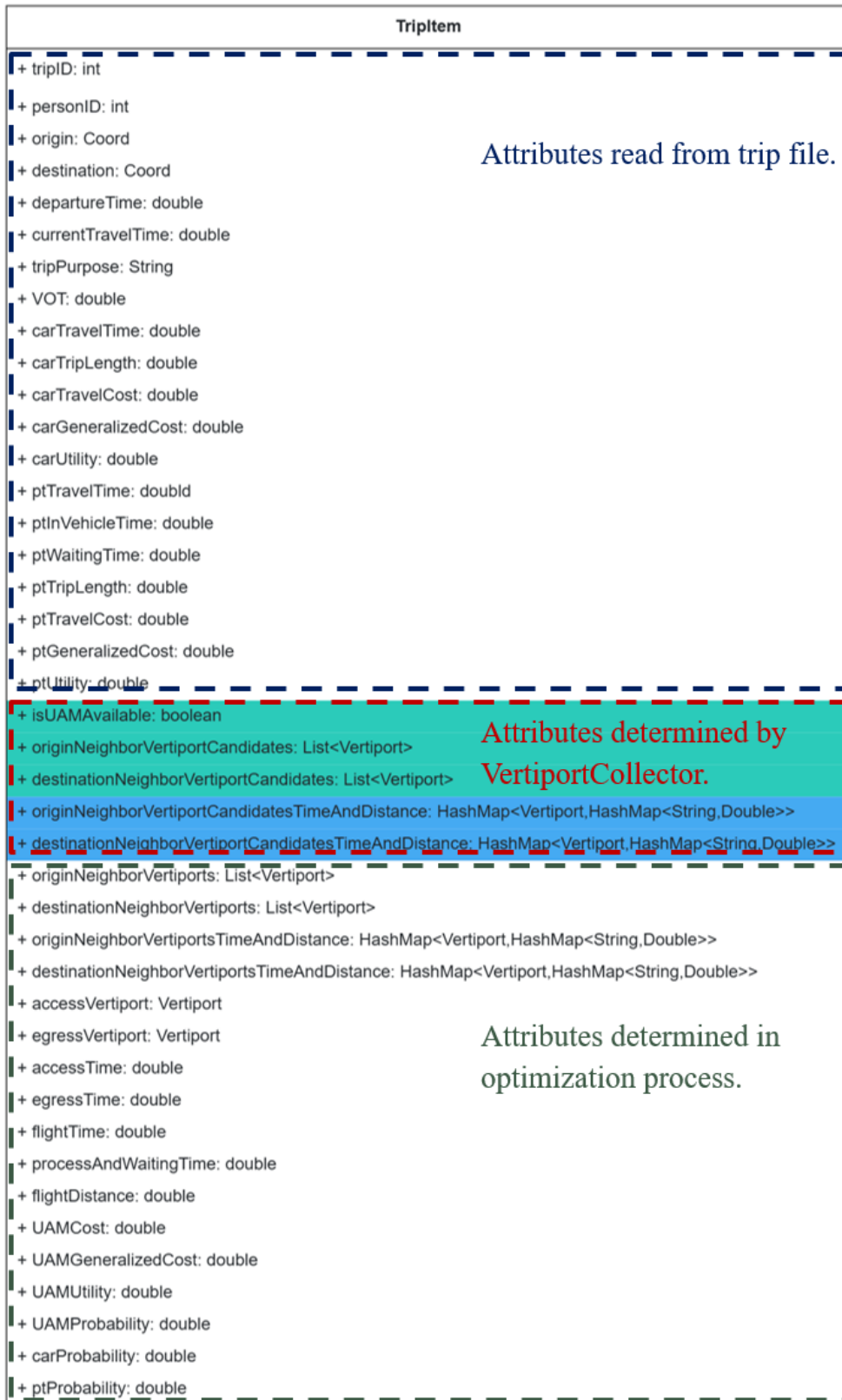
(a) TripItem.

Figure 15 UML diagram of objects TripItem and VertiportCollector.
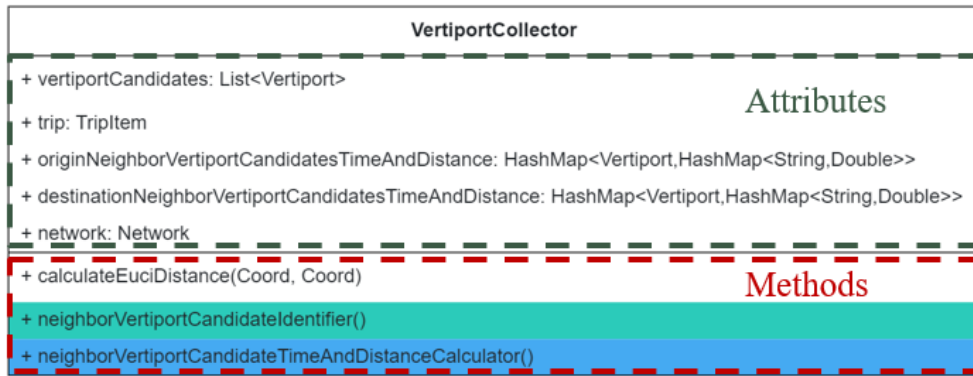
(b) VertiportCollector.

Figure 15 UML diagram of objects TripItem and VertiportCollector (continued).

Since travel time is an essential component in calculating the generalized travel cost of a trip as well as an important attribute in mode choice modeling, it is used in each iteration of optimization in both stages. In order to save the computation resource, the potential travel time of each trip/leg in each mode is pre-calculated. The simulation tool used in this study for calculating the travel time is MATSim, in which a travel time calculator developed by Rothfeld (2021) is available. This calculator requires background traffic for one-time simulation, based on which a "NetworkChangeEvent" file records the network status in each time step could be generated. In MATSim, "NetworkChangeEvent" is a container class for events that represent time-variant changes for link attributes (in SI units) (Horni et al., 2016). Consequently, the framework takes into account potential detours and congestion associated with car and public transportation travel, as well as the scheduling of transit. In the preprocessing step, for each trip, the travel time in each ground transportation mode from origin to destination at a specific departure time could be estimated. Besides, the travel times of the access (egress) legs between the origin (destination) and all vertiport candidates are also calculated for each trip. Then the trip object that contains travel time information is saved as a serialized object file (.dat). The objects involved in the programming implementation are mainly TripItem and VertiportCollector, which contain attributes and methods as shown in Figure 15.

6.4. Parameter Configuration

When adapting the generic optimization formulation to the specific case study, it is essential to define a set of parameters that pertain to the implementation of optimization procedures and UAM operations. In this section, the configurations of these parameters will be explained in detail.

6.4.1. Parameters in Formulation

As delineated in Section 6.2, this case study identifies 200 candidate vertiports. Consequently, the size of the candidate vertiport set, denoted as M, is established at 200. To ensure comparability with previous research (Ploetner et al., 2020; Guo et al., 2024; Arel-

lano, 2020), we have kept the number of vertiports to be selected the same, at 74, i.e., $|V| = 74$. Besides, the search radius for access and egress vertiports are determined as 5 km.

Due to the limitation of trip data and logit model, the available ground-based modes in the case study for pure on-ground trips and access/egress legs of UAM trips are limited to car (both as car drivers and passengers), public transport and walk, i.e. $G, A, E = \{$car, public transport, walk$\}$. When factoring travel time into the generalized cost, the VOT for each trip is estimated based on individuals' income, assuming an annual work time of 2080 hours. Furthermore, the realization of stochastic mode choice variables z is executed by 100 times Monte-Carlo sampling for a trip given a demand-vertiport matching decision.

Table 3 Cost estimation and breakdown of car trips.

Item	Trip Cost (€/ km)	Source Data
Fuel	0.1087	Fuel price: 1.812 €/L (Fleetcor, 2023);
		Fuel Consumption: 6.0L /100 km (Volkswagen, 2023).
Cleaning	0.0560	Cleaning price: 80 €/time (Fleetcor, 2023);
		Frequency: 11.6 times/year (Statistia, 2023);
		Yearly range: 16570 km/year (Held et al., 2021).
Parking	0.0217	Yearly parking cost: 360 €/year (Karowski, 2023).
Insurance	0.0603	Yearly fare: 1000 €/year (ADAC, 2023).
Tax	0.0134	Yearly fare: 222 €/year (Autokosten, 2023).
Depreciation	0.1121	Purchasing price: 33625 €(Volkswagen, 2023);
		Lifespan: 18.1 years (Held et al., 2021).
Interest	0.0205	Assumption: Loan of 20000 €, 10-year term (Sparkasse, 2023).
Maintenance	0.0449	Monthly Cost: 62 €/month (ADAC, 2023).
Sum	0.4376	

6.4.2. Price Schemes of Car and Public Transport

The price schemes of car and public transport trips are determined based on some assumptions and cost structures from previous studies.

- Car: Since the detailed car ownership information (e.g., purchasing price, fuel consumption performance) is not available in the acquired dataset, the car cost is estimated by

taking the Volkswagen Golf 2.0 TDI Comfortline (Volkswagen, 2023) as the model and the cost structure from Lu et al. (2023) as reference. The break-down of cost for car trips is shown in Table 3.

- Public transport: The cost of public transport is estimated under the context of the "Deutschland Ticke" policy in Germany, with which one can unlimitedly travel on regional public transport all over Germany for a monthly fee of 49 €(Bissel, 2023). Consequently, the cost of a public transport trip is estimated as 0.51 €/trip based on the assumption that everyone holds a "Deutschland Ticket" subscription and makes 3.2 trips per day according to MiD 2017 report of Munich (infas et al., 2020).

6.4.3. UAM Operation Parameters and Price Scheme

The technical parameters regarding eVTOL vehicles and operational parameters for UAM service are extrapolated from extant research. To enhance the competitiveness of UAM relative to ground transportation, we selected parameters for the experiment based on high-performance vehicles as delineated in the previous literature. Besides, the range and charg-

Table 4 Overview of UAM-related parameters in the experiment.

Parameter	Existing Value Definition(s)	Value
Processing time+ waiting time	Existing literature defines it as a variable with a wide range, as shown below in minutes: 0, 10, 20 (Ploetner et al., 2020); 0, 10, 30 (Rothfeld, 2021); 0, 4, 8, 12 (Balac et al., 2019).	10 min
VTOL Altitude	When flying over cities and dense areas, aircraft should operate 300 m above the highest obstacle, in other cases, operate at least 150 m above ground level (Bundesamt fuer Jusitz, 2015). For the study area, the height of the Olympic Tower defines it to be at least 591.28 m (Guo et al., 2024).	600 m
Cruise Speed	8 scenarios between 50-350 km/h (Ploetner et al., 2020); 50–200 miles per hour (Wang et al., 2022).	350 km/h
Vertical Speed	Experts consulted the performance benchmark of eVTOL aircraft as 10 m/s (Shamiyeh et al., 2018).	10 m/s
Price	Holden and Goel (2016): 1.5 €/pkm (short term), 0.2 €/pkm (long term); Balac et al. (2019): 6.1 €+ 0.6-4.2 €/pkm; Wu and Zhang (2021): 9.2-27.6 €+ 0.5-1.0 €/pkm; Ploetner et al. (2020): 4.94 €/km.	6.1 €+ 0.6 €/pkm

ing time of eVTOL aircraft are overlooked in this case study since the estimated range could reach 200-300 km due to the enhanced technology, which is already greater than the longest Euclidean distance between any two vertiport candidates in the experiment (165 km) (Swaminathan et al., 2022; Beyne and Castro, 2022). The UAM-related parameters used in the experiment are summarized in Table 4.

6.4.4. Parameters in Heuristic Optimization Algorithms

In this study, the optimization of vertiports siting (outer loop) is achieved by heuristic algorithms. In the five kinds of heuristic algorithms developed and adopted in this study, GA and SA are Meta-Heuristic algorithms, where the relevant parameters need to be defined exogenously and can affect the search efficiency of the algorithms and the quality of the results. In this experiment, the relevant parameters of the Meta-Heuristic algorithms are defined based on trial and error, as shown in Table 5.

Table 5 Parameters in Meta-Heuristic algorithms.

GA		SA	
Parameter	Value	Parameter	Value
Population size	50	Initial temperature	5000
Selection technique	Tournament selection	Cooling rate	0.999
Tournament size	5	End temperature	0.1
Crossover probability	100%	Acceptance probability for worse solution	$e^{-\Delta E/T}$ *
Crossover operation	Single-point crossover	Maximum iteration	10000
Mutation probability	5%	Maximum iteration without improvement	2000
Maximum generation	10000		
Maximum generation without improvement	1000		

*: ΔE: change in energy, T: current temperature.

6.5.   Implementation of Mode Choice Modeling

As stated in problem formulation, mode choice variables, which are treated as stochastic variables in this problem, are generated by discrete choice model and Monte Carlo sampling. The discrete choice model used in this study is developed by Adamidis et al. (2023) based on the stated preference (SP) survey regarding the travel behavior and willingness to use UAM of residents in the catchment area of Munich International Airport, which is roughly the same as the study area in this study. The panel data mixed logit (ML) model is developed to account for the multiple observations from each individual (possible serial correlation) in

the SP experiment. Among all models in the study by Adamidis et al. (2023), the ML model illustrates the best performance regarding the Adj. Rho-Square. The ML model is shown in Appendix A. The reported estimation results include statistically significant coefficients at a 10% significance level, with the alternative specific attributes having been scaled (reduced) by a factor of 100. Unfortunately, due to limitations in the survey questions, the ML model cannot encompass the modeling of access and egress modes. In other words, the nested logit model is not available. Therefore, during the experimental process, the probability estimation and Monte Carlo can only be performed for the main transport mode. Access and egress mode choices are simplified to selecting the one with the lowest generalized travel cost. The process of mode choice modeling is illustrated in Figure 16.
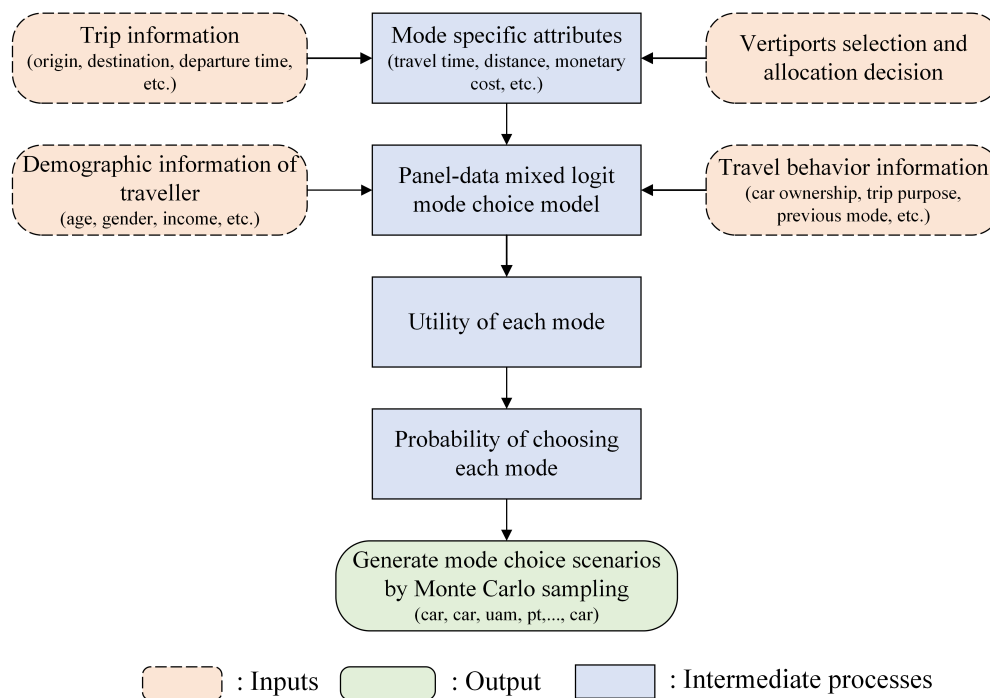
Figure 16 Process of mode choice modeling for one trip.

7. Results Analysis

7.1. Vertiports Layouts

(a) GRDF solution.

(b) GRDF-U solution.

(c) GRDB solution.

(d) GA solution.
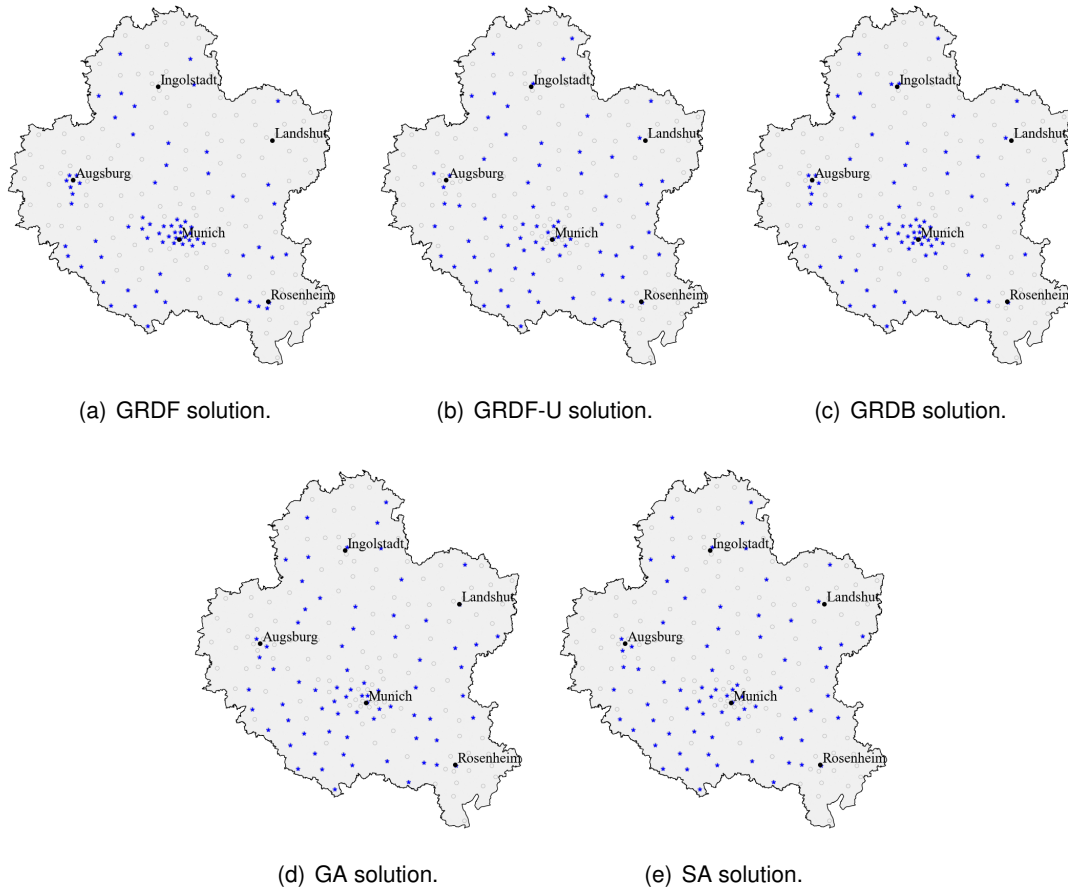
(e) SA solution.

Figure 17 Selected vertiports in all solutions.

After conducting the experiments, each optimization algorithm eventually yielded the corresponding vertiports placement results. The vertiports layouts of these five solutions are shown in Figure 17. Obviously, the three algorithms GRDF-U, GA, and SA obtained remarkably similar solutions. Among the 74 vertiport locations identified, 60 were consistent across all these three solutions. On the other hand, the solutions obtained by the GRDF and GRDB algorithms are also highly similar, with 61 vertiports overlapping between the two. In terms of the geographical distribution of vertiports, the GRDB and GRDF solutions tend to place vertiports more concentrated in the vicinity of the municipal area of Munich. Furthermore, the Augsburg neighborhood also has a considerable number of vertiports, while the rest of the region is very sparsely settled. In contrast, the GRDF-U, GA, and SA solutions tend to distribute vertiports more evenly throughout the study area. Although there are indeed relatively more vertiports near major cities (e.g., Munich, Augsburg) compared to rural areas. It is worth noting that vertiports are fairly concentrated near the southwest corner (e.g.,

Landsberg, Weilheim) of the study area in all solutions. Furthermore, the vertiport placement schemes manually selected by experts in the OBUAM project (Ploetner et al., 2020) and generated by clustering methods (Guo et al., 2024) are used as benchmarks to compare with the optimization methods used in this study. The vertiports displacement schemes from benchmarks are shown in Appendix B for reference.

7.2.   Optimization Performance Evaluation

Table 6 Saved generalized travel costs and computation time in each solution for the comparison with benchmarks.

Algorithm	Saved Generalized Travel Cost (€)	Computation Time (min)	Source
GRDF*	32521.2	12.17	Willey and Salmon (2021)
GRDF-U**	**41387.8**	33.67	own development
GRDB**	35374.7	0.02	own development
GA	**41316.1**	342.36	-
SA	**41657.9**	15.15	-
Benchmarks from preliminary studies			
OBUAM	15484.3	-***	Ploetner et al. (2020)
DBSCAN	9456.7	-	Guo et al. (2024)
KM++	**29068.9**	-	Guo et al. (2024)
KM$_{OBUAM}$	24065.1	-	Guo et al. (2024)
GMM++	18564.5	-	Guo et al. (2024)
GMM$_{OBUAM}$	27839.4	-	Guo et al. (2024)
HC	26355.6	-	Guo et al. (2024)
MS	22227.5	-	Guo et al. (2024)

Note: *: The algorithm is adapted from others. **: The algorithms are developed by the authors of this research. ***: Computation time is not mentioned in the source papers.

As a large-scale network NP-hard problem, the global optimal solution can only be found by exhaustively trying all possible solutions (Willey and Salmon, 2021). All heuristic algorithms cannot guarantee the global optimal solution but aim to get as close to it as possible. Therefore, we compare the solutions obtained by these algorithms and their corresponding objective function values (i.e., saved generalized travel costs) to assess the quality of the solutions. The results are presented in Table 6.

Subsequently, the optimization results are compared with the benchmarks. The trips, demand allocation, and mode choice modeling processes used in the optimization approaches are exactly the same as in this experiment. The results are also presented in Table 6 and show that the solutions obtained by all optimization algorithms lead to significantly greater saved generalized costs compared to the benchmarks' solutions. This demonstrates the superiority of the optimization methods.

As is convention in optimization algorithm-related research, computation time is also an important metric for evaluating algorithms. The computational experiments were conducted on a high-performance system powered by a 13th Gen Intel(R) Core(TM) i7-13700K processor. This processor, belonging to the x86_64 architecture, operates with 24 CPUs (0-23 online). It has a maximum frequency of 5400 MHz and a minimum of 800 MHz. The system is equipped with a substantial 125 GB of RAM. This setup runs on Ubuntu 22.04.3 LTS, which ensures a stable and efficient operating environment for the algorithms' performance evaluation. As shown in Table 6, the computation times for all the algorithms are within an acceptable range. As expected, the GRDF and GRDB algorithms run quickly. The GRDB algorithm runs extremely fast because it only performs one-time saved generalized cost calculations (for all trips) for exactly one network. GRDF-U and SA algorithms have slightly longer computation times. GA has the longest computation time because it requires fitness calculations for every chromosome in the population in each iteration. For more information on the evolutionary processes of the GA and SA algorithms, refer to Figure 18.

(a) Best fitness change in GA. (b) Temperature and best energy change in SA.
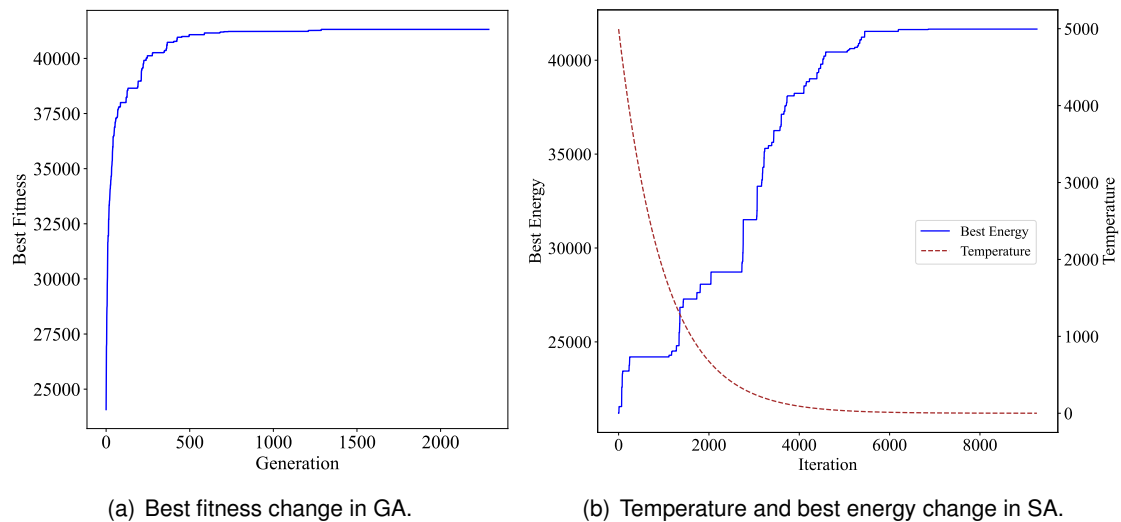
Figure 18 Evolution processes in GA and SA.

Similar to the comparison of vertiport layouts, the objective function values for GRDF and GRDB solutions are very close, while the solutions for GRDF-U, GA, and SA are also very close to each other but significantly surpass the former two solutions. It is evident that the simple Greedy algorithm, whether forward or backward, struggles to efficiently produce solutions close to the global optimum. The GRDF-U algorithm brings about a significant improvement in the results. The more advanced meta-heuristic algorithms (GA and SA) also

generate superior solutions compared to the simple Greedy algorithm.

7.3. Demand Coverage Assessment

Although demand coverage is not the primary objective of the p-hub location problem, it has a crucial impact on the UAM service level. Therefore, this study also includes it in the evaluation for vertiport placement.

Table 7 Demand coverage, and weighted average accessibility improvement ratio (definition in Section 7.4) in each solution for the comparison with benchmarks.

Algorithm	Demand Coverage Rate (%)	Weighted Average r_{ai} (%)	Source
GRDF	34.3	6.0	Willey and Salmon (2021)
GRDF-U	**50.8**	**7.7**	own development
GRDB	39.5	**7.7**	own development
GA	**51.3**	**7.9**	-
SA	**50.9**	**7.9**	-
Benchmarks from preliminary studies			
OBUAM	27.2	4.3	Ploetner et al. (2020)
DBSCAN	28.4	4.2	Guo et al. (2024)
KM++	**52.0**	5.8	Guo et al. (2024)
KM$_{OBUAM}$	46.5	4.5	Guo et al. (2024)
GMM++	37.1	**6.0**	Guo et al. (2024)
GMM$_{OBUAM}$	45.5	4.4	Guo et al. (2024)
HC	47.6	5.4	Guo et al. (2024)
MS	32.4	5.4	Guo et al. (2024)

As shown in the second column of Table 7, GRDF and GRDB algorithms still have unsatisfactory performance in terms of demand coverage, with both having coverage rates below 40%. On the other hand, the remaining three solutions are still similar and superior, with coverage rates exceeding 50%. When compared to the benchmarks, it can be observed that while the KM++ solution generated by clustering outperforms the optimization solutions, considering that clustering methods are demand-oriented in nature and only slightly better, the optimization solutions can still be considered promising concerning demand coverage.

Figure 19 illustrates the demand coverage ratio for each zone, in which areas where there is a clear difference are highlighted with blue circles. Clearly, the solutions from GRDF-U, GA, and SA cover a broader range of areas with their vertiports' service areas. Particularly, in the southwestern part of the study area (Weilheim) (shown by the middle blue circle in the figures) and the rural area between Munich and Augsburg as well as the counties around Rosenheim, the demand coverage rates in GRDF-U, GA and SA solutions are significantly superior compared to the results from GRDF and GRDB.

(a) GRDF   (b) GRDF-U   (c) GRDB

(d) GA   (e) SA   (f) Legend
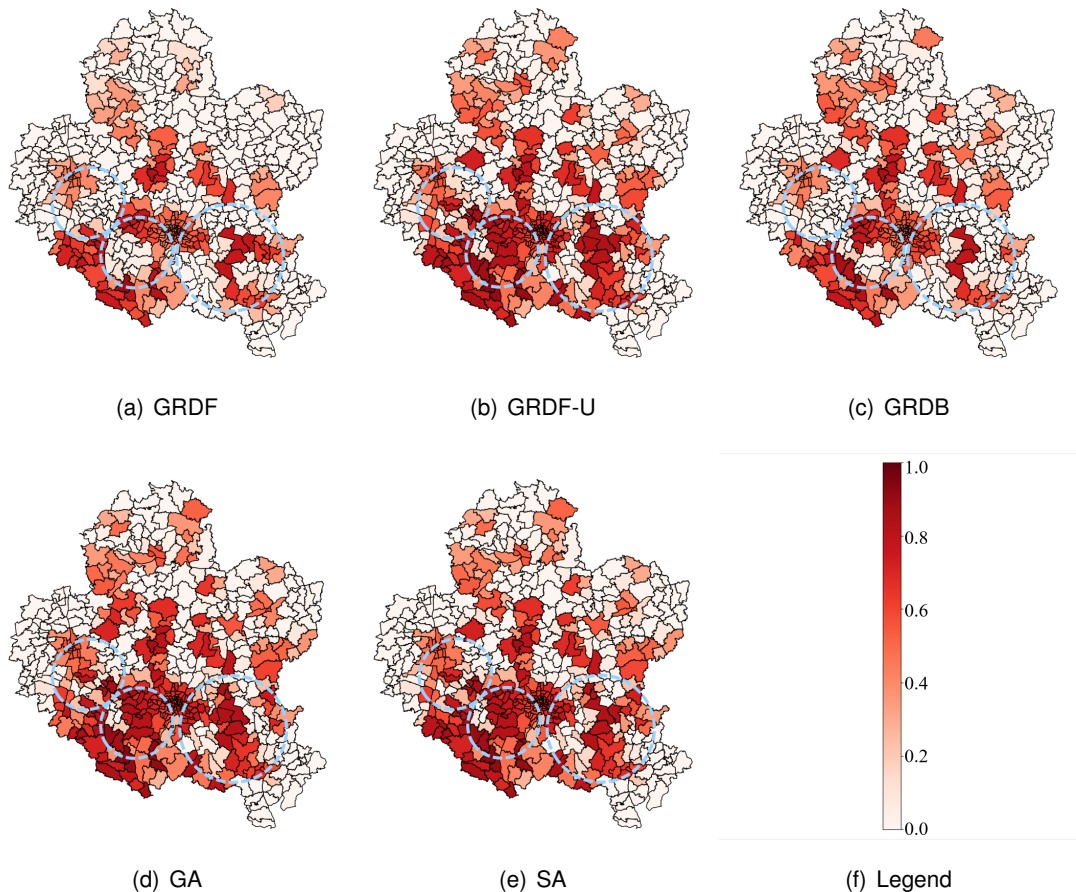
Figure 19 Vertiports demand coverage ratio in all solutions.

7.4. Accessibility Improvements Assessment

The accessibility measure chosen in this study is a cumulative opportunities measure, as defined by Geurs and Van Wee (2004), which was also adopted in many reference papers (Rothfeld, 2021; Guo et al., 2024). The quantified accessibility is calculated by taking cumulative opportunities and travel costs into a gravity negative-exponential model. In the case of this study, the number of opportunities was measured in terms of the number of activity opportunities including job, education, and amusement opportunities at the destination zone, whereas the impedance is measured by travel time between zones, which is consistent as the work by Rothfeld (2021) and Guo et al. (2024). For a given zone i, the accessibility level

Figure 20 Cumulative frequency of accessibility improvement ratio.

is equal to the sum of job opportunities to all other zones by counting the diminishing effects of opportunities requiring longer travel time. The definition is mathematically expressed in Equation (7.1),

$$A_i = \sum_{j=1}^{n} D_j e^{-\beta c_{ij}} \tag{7.1}$$

where, A_i is the quantified measure of accessibility in zone i, n is the number of zones, D_j is the number of opportunities in zone j, c_{ij} is the generalized cost for trips from zone i to j, β is the cos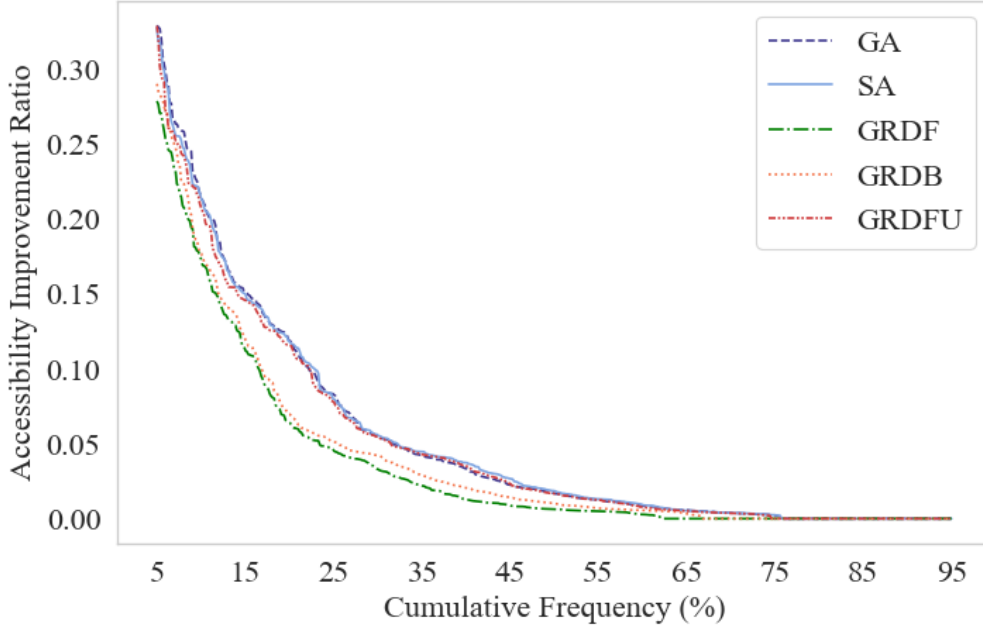t sensitivity parameter, which was according to Rothfeld (2021) set as 0.2. The accessibility of each zone with ground-based transportation modes and UAM is calculated and compared. The accessibility improvements ratio r_{ai} is calculated accordingly. The accessibility in this context is zone-based. Thus, from a macroscopic level, a decrease in accessibility after the introduction of UAM makes no sense, and therefore, r_{ai} is set to 0, correspondingly. The mathematical expression is shown in Equation (7.2).

$$r_{ai} = \frac{A_{uam}}{A_g} - 1 \tag{7.2}$$

The weighted average accessibility improvement ratio among all zones of each solution is shown in the third column of Table 7. The weight of each zone is determined by the number of opportunities. The results yield a promising overall accessibility improvement brought by all solutions. When compared to benchmarks, it can be seen that the weighted average r_{ai} of the solutions produced by all the optimization methods outperform benchmarks, which again proves the superiority of the optimization method. Among the optimization solutions, GRDF-U, GA, and SA still show superior enhancement levels compared with the GRDF solution. Unexpectedly, the weighted average r_{ai} of GRDB solution is also significantly higher than that

of GRDF. One possible reason for this is that this average is more influenced by individual zones with exceptionally high r_{ai}. Therefore, to eliminate the effect of extreme values, we sorted all zones in each solution based on r_{ai} and extracted zones within the 5%-95% interval to plot the cumulative distribution, as shown in Figure 20, from which, it can be seen that the GA, SA, and GRDF-U solutions perform better than GRDF and GRDB in terms of overall accessibility enhancement.
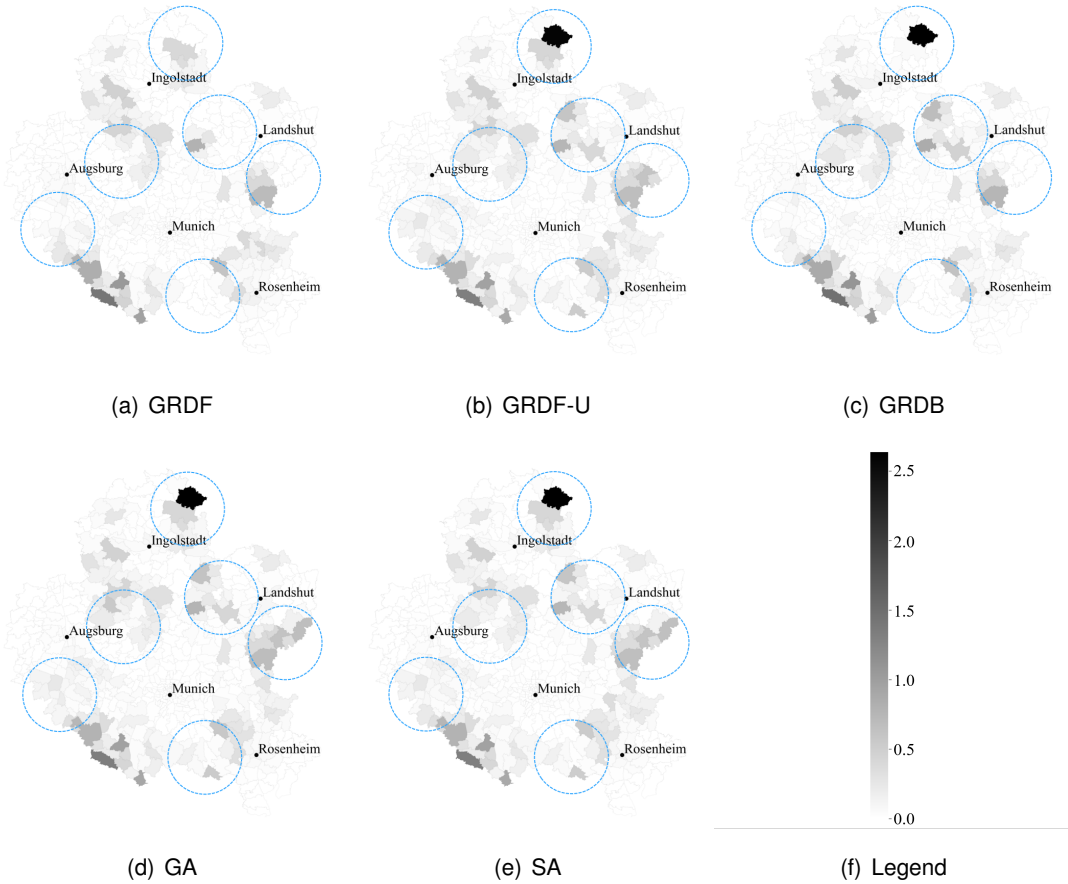
Figure 21 Accessibility improvement ratios of zones.

In addition to the degree of accessibility improvement, its geographical distribution is also of concern. Figure 21 shows the distribution of accessibility improvements in different zones for various solutions. The areas that yield significant differences are also encircled in blue. Similar to the conclusion drawn by Guo et al. (2024), all solutions do not provide significant accessibility improvements to major cities (especially Munich). One possible reason is that for residents in major cities, their primary opportunities are limited to the local urban area, and the travel needs concerning the opportunities are primarily short-distance. Almost all previous research on UAM supports the idea that UAM is not competitive compared to cars for short-distance trips. Therefore, UAM may not bring significant accessibility improvements to major cities overall. In a cross-comparison of the solutions, GA, SA, and GRDF-U still bring greater accessibility improvements to rural and suburban areas, as shown in Figure 21.

7.5. Sensitivity Analysis of the Number of Vertiports

All the experiments and results assessments mentioned above were based on a fixed number of vertiports. The reason for choosing 74 vertiports in the experiment is to facilitate comparison with benchmarks provided by previous studies, as explained in parameter configuration (Section 6.4). However, in practice, when conducting vertiport siting studies in a new area, such knowledge is often unavailable, and determining the appropriate number of vertiports can be challenging. In transportation engineering projects, cost-benefit analysis (CBA) is a commonly used method for construction-related decision-making (Damart and Roy, 2009). This can be achieved by changing the formulation and treating the number of vertiports (p) as a decision variable to be determined by the optimization results. In this case, it is necessary to introduce terms related to cost in the objective function to prevent the number of vertiports from growing indefinitely. However, based on existing research results, the estimates for vertiport construction and operation costs are rough, and the relationship between cost and saved generalized travel cost (benefits) has not been thoroughly studied. Therefore, it is almost impossible to determine the weights of both objectives in the formulation. Hence, in this study, the authors used a qualitative approach to discuss the relationship
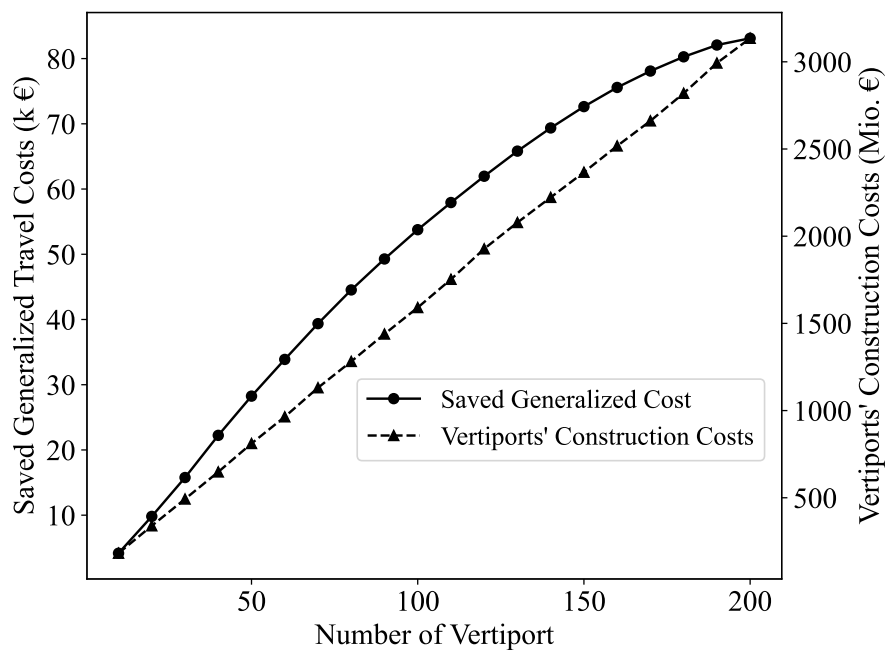
Figure 22 Saved generalized travel cost and construction cost across various numbers of vertiports.

between the number of vertiports and costs, as well as benefits. Subsequently, a series of exploratory optimization experiments were conducted with the number of vertiports set to start from 10 and increment by 10 up to 200. The SA approach, which has performed well in terms of optimization results and computation time, was used. The approximate construction costs of vertiports were estimated based on the cost structure by Malaek et al. (2019) (shown in Appendix C) and the local land price data from Immoportal (2023) (shown in Appendix D). The estimated cost for building a vertiport in each county is shown in Appendix

E. The objective function value and total vertiport construction cost in each experiment are shown in Figure 22. It is evident that with the increasing number of selected vertiports from the given vertiport candidates, saved generalized travel costs continue to increase, but the rate of increase tends to slow down. This validates the diminishing marginal utility in the context of vertiport siting (Easterlin, 2005). On the other hand, although the construction costs of vertiports at different locations vary significantly, the growth of total cost with an increasing number of selected vertiports remains approximately linear. This demonstrates that having an excessive number of vertiports is not cost-effective, and it also indicates that there is an equilibrium between saved generalized travel costs and construction costs, although this point cannot be quantitatively determined at present due to data deficiency in infrastructure cost estimations.

8. Limitations

In terms of framework building, like many similar studies (Willey and Salmon, 2021; Wu and Zhang, 2021), this research framed the problem as an uncapacitated hub location problem, which did not account for the capacity of vertiports and the availability of eVTOL aircraft. As a result, dynamically modeling travelers' waiting times at vertiports and the interactions between travelers, stated in Husemann et al. (2023), was not achieved. This limitation can potentially impact the results, as demand allocation and mode choice may yield different outcomes when vertiports lack available vehicles or require longer waiting times. Addressing this issue will be a focus of future research.

Furthermore, some limitations regarding the experiment were brought about by the shortage and constraints of available data. On one hand, due to constraints in trip data and the logit model, this experiment could not include additional ground-based transport modes such as car sharing, bicycles, e-bikes, and taxis. Since the survey in Adamidis et al. (2023) yielded the conclusion that the shares of those modes are relatively low, the overlook of those modes might not have significant influences on the optimization results. Additionally, the absence of a nested mode choice model prevented the simulation of access and egress mode choices for UAM trips, restricting the choice to the mode with the lowest generalized cost. This compromise introduced some bias into the experimental results compared to real-world scenarios. On the other hand, due to the lack of accurate cost estimation from existing literature, such as public transport travel cost, UAM price, and vertiports construction cost, the cost-related parameters configuration for the economic evaluation were estimated roughly. In the future, when more research and data on these topics are available, more accurate calculations will become possible.

Finally, in the experiments, the calculation of travel time for ground-based trips did not consider the impact of the introduction of UAM on existing ground transportation. According to Wang and Qu (2023), the induced traffic in the vicinity of vertiports, resulting from the access and egress legs of large-scale UAM applications, will inevitably exacerbate congestion in these areas. The omission of this effect from our model was due to the limited share of UAM potential trips, which constitute less than 1% of all trips, as highlighted in the study by Ploetner et al. (2020). Furthermore, the implementation of traffic simulations, particularly those using MATSim, requires significant computational resources for each scenario. In future works, enhanced simulation speeds or advanced simulation tools may enable more realistic travel time calculations, incorporating the effects of UAM on ground traffic.

9. Conclusions and Policy Insights

9.1. Conclusions

This study addresses the UAM vertiports siting problem by constructing a two-stage stochastic optimization model to determine the optimal subset of selected vertiports from a given set of vertiport candidates. In this framework, the decision variables in the first stage are the vertiport selections, and in the second stage, the decision variables are the matching of trip origins and destinations with vertiports (demand allocation). To achieve a more realistic and accurate simulation of travelers' transport mode choice, mode choice is included in the framework as a stochastic variable in the objective function. Its realization relies on the probabilities computed by the discrete choice model and Monte Carlo sampling. From an optimization algorithm perspective, the inner loop (demand allocation) of this framework is achieved through enumeration, assuming that each trip is independent of others. The outer loop (vertiport siting) is optimized using five different heuristic algorithms, namely GRDF, GRDF-U, GRDB, GA, and SA.

Subsequently, numeric experiments were conducted using the Munich metropolitan area as the study area. In this region, 200 vertiport candidates were identified using the K-means++ clustering method. The optimization algorithm will select 74 vertiports from these candidates. Although heuristic algorithms cannot guarantee global optimal solutions, carefully designed and tuned algorithms can provide close to optimal solutions within acceptable computation time. In terms of optimization results, the saved generalized travel costs obtained by the GRDF-U, GA, and SA solutions are significantly better than those of the GRDF and GRDB solutions, and these three solutions are quite close to each other. This suggests that approximate optimal solutions have been obtained. Furthermore, when compared to benchmarks obtained from previous studies, it can be seen that the solutions obtained through optimization methods clearly result in more significant savings in generalized travel costs. This also demonstrates the effectiveness of the optimization algorithms. The computation time for all algorithms is generally acceptable.

In addition to the most straightforward criterion, i.e., objective function values, this study also evaluates the various solutions in terms of demand coverage and accessibility improvement. To more intuitively illustrate the differences between the results, demand coverage ratios and accessibility improvement ratios are presented in a zone-based format. In terms of demand coverage, GRDF-U, GA, and SA still perform excellently, with demand coverage rates exceeding 50% across the entire area, comparable to the best benchmarks. On the other hand, GRDF and GRDB fall short, with an overall demand coverage rate of less than 40%. Looking at the distribution in various zones, the vertiports layouts yielded from GRDF-U, GA, and SA can serve more zones, particularly those located southwest of the study

area. Regarding accessibility, the results show that GRDF-U, GA, and SA outperform the other two solutions in terms of both the extent of accessibility improvement and the breadth of benefiting areas. They can provide over 5% accessibility improvement for approximately 30% of all zones.

Finally, to explore the impact of the number of vertiports, the authors conducted exploratory experiments where the number of vertiports ranged from 10 to 200. The findings indicated that while the overall savings in generalized travel cost escalated with the addition of vertiports, a pronounced diminishing marginal effect was observed, characterized by a deceleration in the rate of increase. On the other hand, based on the author's estimate of each vertiport's construction cost, the total construction costs of vertiport siting schemes for different numbers of vertiports were calculated. It essentially increased linearly with the number of vertiports. This provides a foundation for future cost-benefit analyses to determine the optimal number of vertiports.

In conclusion, the two-stage optimization framework designed in this study has been validated through experiments and demonstrated superior performance in various aspects compared to benchmarks.

9.2. Policy Insights

In the concluding section (Section 9.1), the paper synthesizes the intuitive insights derived from the experimental outcomes and exploratory research. This section will discuss the contributions of this study's findings from the policy-making perspective, highlighting how it informs policy decision-making. As introduced before, UAM holds the potential to revolutionize urban transportation. The strategic siting of vertiports is central to unlocking this potential, offering a range of societal and economic benefits.

When planning a UAM network for a new area, policymakers often have a predetermined budget for the total construction cost of vertiports. Consequently, the number of vertiports is usually pre-established (refer to Figure 22), consistent with the scenario outlined in this study. The two-stage stochastic optimization model introduced here provides optimal vertiport siting solutions, resulting in significant generalized travel cost savings, increased demand coverage, and enhanced accessibility and transport equity.

- Substantial Reductions in Travel Costs: In this study, travel-related costs are encapsulated by the concept of "generalized travel cost", which encompasses both monetary expenses and travel time. This metric serves as a crucial indicator for assessing the social benefits of UAM. The experimental results demonstrate that our proposed model, aimed at optimizing the total generalized travel cost, significantly reduces total expenses compared to traditional ground transportation. Moreover, the effectiveness of our optimization methods

is further underscored when compared to previous studies with an equivalent number of vertiports.

- Enhanced Demand Coverage: Strategic placement of vertiports significantly broadens the service coverage of UAM, thereby extending its benefits to a larger portion of the population. This expansion makes UAM a more inclusive and extensively utilized mode of transportation. Although not the primary focus of this optimization problem, the optimization-based approach for vertiport placement has also demonstrated effective demand coverage. Compared to benchmarked methods, these optimization techniques maintain robust performance. This strategy is particularly valuable in densely populated regions where the need for efficient transportation solutions is paramount.

- Enhanced Accessibility and Transport Equity: The proposed UAM siting model significantly improves access to various activity opportunities, thereby augmenting regional economic benefits following the introduction of UAM services. In addition to its primary objective, the optimization process also achieves notable gains in accessibility. Experimental results indicate that certain optimization solutions yield an approximate 8% increase in weighted average accessibility across different zones, surpassing the typical 5% fluctuation observed in benchmarks. This enhancement is particularly vital for promoting transport equity, especially in communities historically underserved by conventional transportation systems. Establishing vertiports in these areas can offer more efficient mobility options, playing a key role in bridging the urban mobility divide.

When devising regional UAM networks, policymakers sometimes also confront uncertainties concerning the precise number of vertiports required. Their decision-making process frequently involves a careful evaluation of the potential benefits in relation to the incremental costs associated with varying numbers of vertiports. To address this issue, our study offers pertinent policy insights.

- Marginal Diminishing Effect of Benefits: While this study does not perform a quantitative Cost-Benefit Analysis (CBA) on the number of vertiports, it qualitatively illustrates the relationship between the savings in generalized travel costs, the estimated construction costs, and the number of vertiports. This relationship highlights a marginal diminishing effect of benefits. Specifically, as the number of vertiports escalates, there is an increase in the generalized cost savings from optimized siting, but this increase exhibits a decelerating rate. In contrast, the construction costs tend to rise almost linearly with each additional vertiport.

From a practical perspective, the vertiport siting methodology proposed in this study is generalizable, and its reliance on straightforward data significantly reduces the necessity for extensive expert input, which can be prohibitively costly in certain regions. Heuristic algorithms ensure that the solutions approach near-optimality and maintain computational efficiency, even when processing extensive datasets like the disaggregated travel demand analyzed in

this study. This approach is instrumental in facilitating UAM network planning and lays a foundation for subsequent research in the field.

Appendices

A. Panel Data Mixed Logit (ML) Model

The panel data mixed logit model shown in Table A.1 is developed by Adamidis et al. (2023) based on their SP survey conducted in the same area as in this thesis.

Table A.1 Panel data mixed logit (ML) model.

Parameters (β_i)	Car			Public Transport			UAM		
	Value	Rob. stat.	T-	Value	Rob. stat.	T-	Value	Rob. stat.	T-
ASC	8.11***	4.45		0	-		8.77***	6.06	
$Travel\ cost$	-6.36***	-5.44		-6.36***	-5.44		-2.48***	-8.02	
$In-vehicle\ time$	-7.98***	-6.26		-4.28***	-3.82		-4.28***	-3.82	
$Waiting\ time$	-	-		-	-		-6.79***	-4.22	
Travel behavior									
$Car\ ownership$	-	-		-	-		-1.28*	-1.84	
$Previous\ mode_{Car}$	1.26*	1.85		-	-		-	-	
$Previous\ mode_{PT}$	-	-		4.11***	4.31		1.98**	2.56	
$Business\ trip$	-	-		-	-		1.83**	2.38	
Sociodemographics									
$Age \geq 50$	-	-		-	-		-0.94**	-2.33	
$Household\ income < 3000$ €	-	-		-	-		-0.76*	-1.93	
$Household\ income \geq 7000$ €	-	-		-	-		3.33**	2.14	
$ASC(\sigma_{error})$	2.47***	5.56		2.55***	5.45		-	-	
Summary of statistics									
No.of observations	1280	LL(0)	-1406.22						
Adj. Rho-Square	0.65	LL(final)	-476.53 AIC	987.05		BIC	1044.59		

Significance levels (Rob.p-value): 0'***', 0.01'**', 0.05'*', 0.1

B. Vertiports Layouts of Benchmarks

Figure B.1 indicate the vertiport layouts schemes from Ploetner et al. (2020) and Guo et al. (2024).
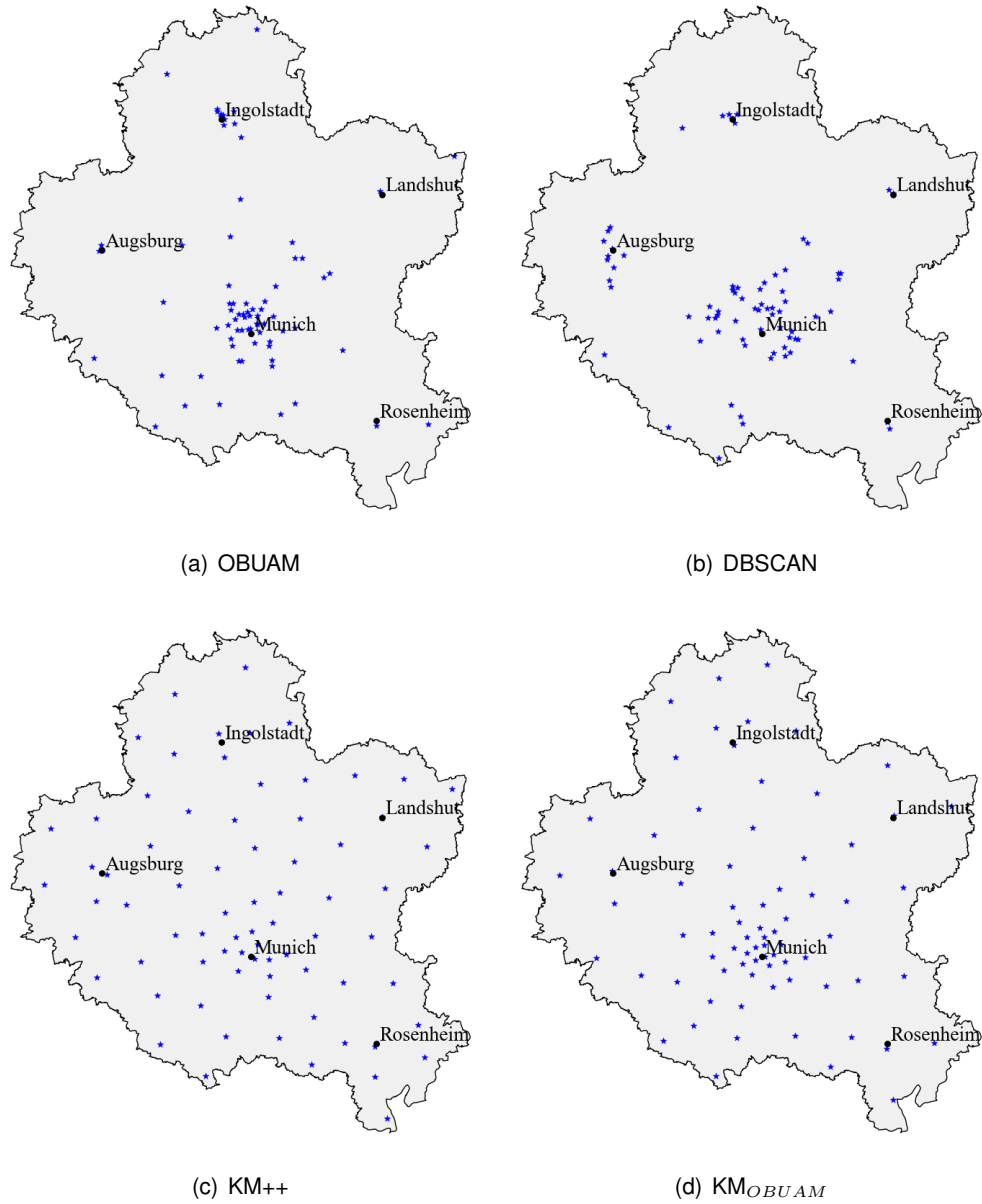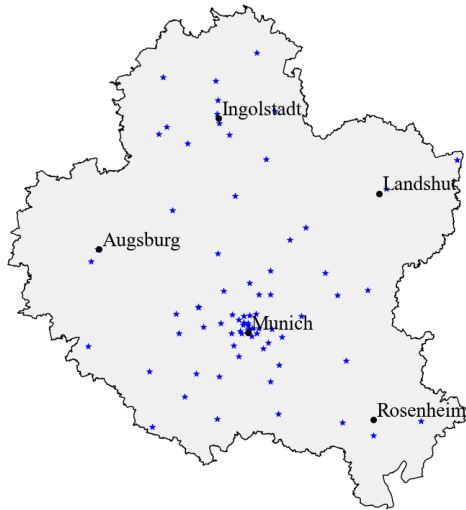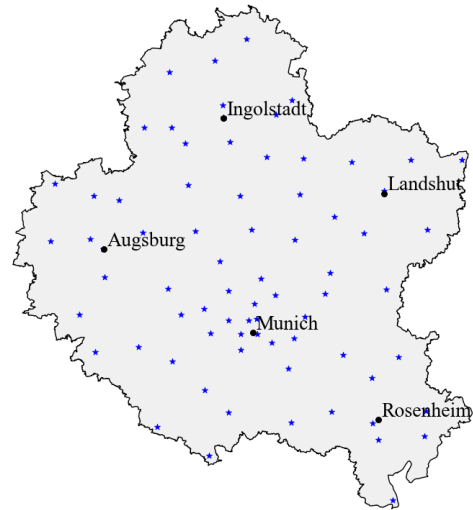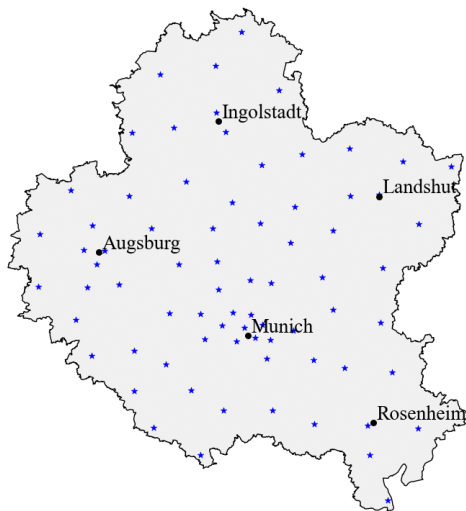

(a) OBUAM

(b) DBSCAN

(c) KM++

(d) KM$_{OBUAM}$

Figure B.1 Vertiports layouts of benchmarks.

(e) GMM++

(f) GMM$_{OBUAM}$

(g) HC

(h) MS

Figure B.1 Vertiports layouts of benchmarks (continued).

C. Break-down of Vertiport Construction Cost

The cost structure is derived from the work by Malaek et al. (2019). Table C.1 presents the converted currency in €.

Table C.1 Break-down of vertiport construction costs.

Item	Cost Per Unit ($)	Cost Per Unit (€)	Quantity	Subtotal (€)
Station for landing and take-off	37100	34503*	6	207018
Chargers	1200	1116	1500	1674000
Robotic Lift Truck	15000	13950	12	167400
Elevator	50000	46500	2	93000
Hydraulic lift equipment for batteries	5000	4650	60	279000
Portable Foam Unit	1000	930	3	2790
Safe Melt	65	60.45	10	604.5
Perimeter Light	575	534.75	96	51336
Flood Light	595	553.35	24	13280.4
Light Control Unit	4425	4115.25	2	8230.5
Weather Station	5450	5068.5	1	5068.5
Wind Cone	3200	2976	1	2976
Light Replacement	405	376.65	30	11299.5
Crash Rescuer Locker	2250	2092.5	2	4185
Hydraulic Power Cutting	4250	3952.5	2	7905

Table C.1 continued from previous page

Item	Cost Per Unit ($)	Cost Per Unit (€)	Quantity	Subtotal (€)
First Air Kit	950	883.5	8	7068
Trolling Case with Tools	3400	3162	2	6324
Surge Protector	2300	2139	2	4278
Portable Lighting System	8950	8324	2	16647
Stretcher (ST66011)	190	176.7	6	1060.2
Ambulance Stretcher	500	465	6	2790
Construction Cost		163**	10740***	1750553
Land price		268****	10740	2878320
Total				7195024

Note:

*: 1 US $=0.93 €.

**: Average material cost in Germany (Statista, 2022).

***: In source paper the area of the vertiport is estimated as 115600 square feet.

****: Take the average land price in Neumarkt i.d. OPf. as an example. The land price in each county will be shown below.

D. Land Price of Each County in MUC

The land price in 2023 is captured from the "Immoportal" website (Immoportal, 2023).

Table D.1 Land price of each county in MUC.

County	Land Price (€/m^2)	County	Land Price (€/m^2)
Neumarkt i.d. OPf.	268	Dachau	992
Eichstätt	265	Freising	864
München	3840	Erding	960
Kelheim	288	Mühldorf a. Inn	307
Ingolstadt	768	Lkr.München	1632
Neuburg-Schrobenhausen	320	Ebersberg	576
Pfaffenhofen a.d. Ilm	467	Fürstenfeldbruck	1136
Lkr. Landshut	540	Landsberg am Lech	576
Landshut	640	Starnberg	1504
Dingolfing-Landau	300	Lkr. Rosenheim	515
Dillingen a.d. Donau	160	Rosenheim	704
Lkr. Augsburg	610	Weilheim-Schongau	684
Augsburg	896	Bad Tölz-Wolfratshausen	1024
Aichach-Friedberg	364	Miesbach	1024

E. Estimated Cost for Constructing a Vertiport in each County

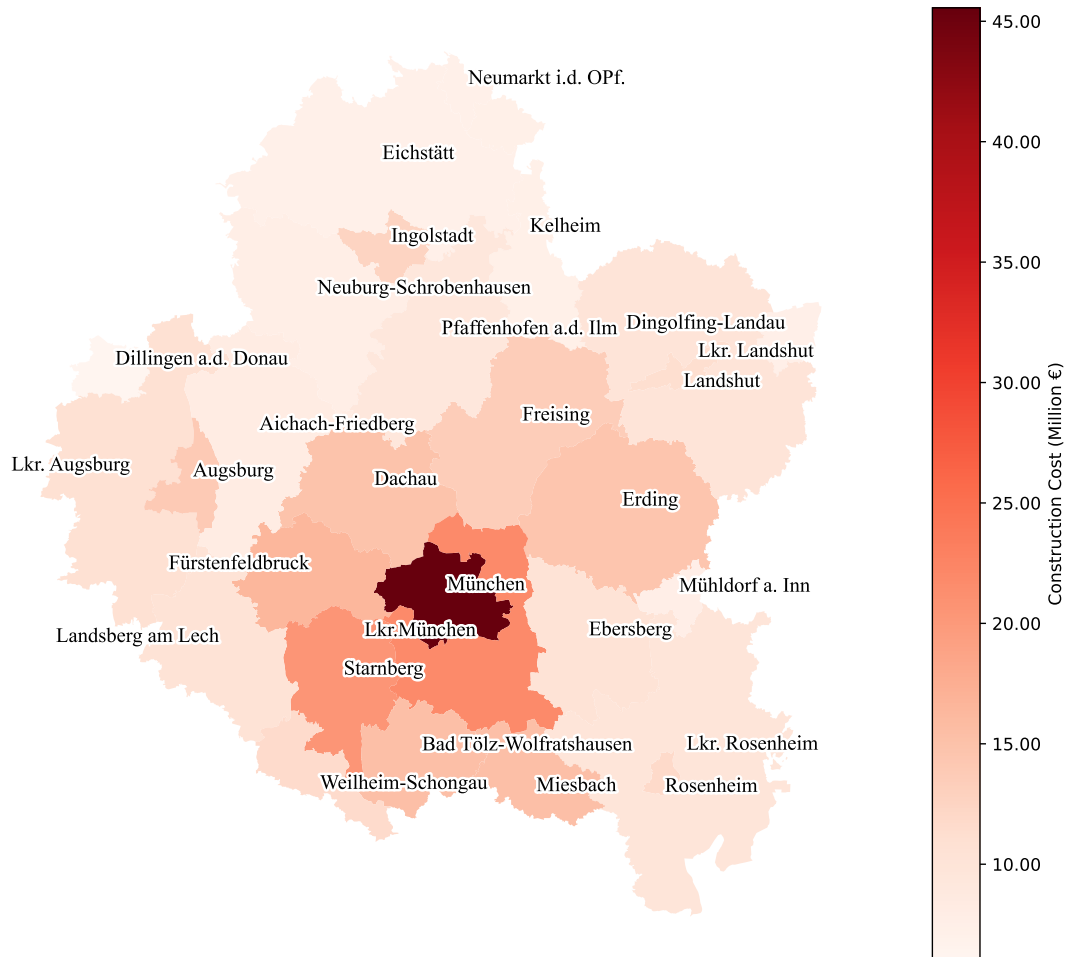Figure E.1 illustrates the construction cost for a single vertiport in each county within the study area.

Figure E.1 Estimated vertiport's construction cost in each county.

Bibliography

ADAC, 2023. Übersicht: Autokosten von A bis Z. https://www.adac.de/rund-ums-fahrzeug/auto-kaufen-verkaufen/autokosten/uebersicht/. Accessed: 2023-10-14.

Adamidis, F., Ditta, C.C., Wu, H., Postorino, M.N., Antoniou, C., 2023. Urban Air Mobility for Airport Access: Mode Choice Preferences and Pricing Considerations. Under Review .

Alumur, S., Kara, B.Y., 2008. Network Hub Location Problems: The State of the Art. European Journal of Operational Research 190, 1–21. doi:10.1016/j.ejor.2007.06.008.

Antcliff, K.R., Moore, M.D., Goodrich, K.H., 2016. Silicon Valley as an Early Adopter for On-Demand Civil VTOL Operations, in: 16th AIAA Aviation Technology, Integration, and Operations Conference, American Institute of Aeronautics and Astronautics. p. 3466. doi:10.2514/6.2016-3466.

Arellano, S., 2020. A Data- and Demand-Based Approach at Identifying Accessible Locations for Urban Air Mobility Stations. Master's thesis. Technical University of Munich.

Autokosten, 2023. Kfz-Steuer VW Golf VI. Golf 2.0 TDI HSN:0603 / TSN:ALT 2016. https://www.autokosten.net/vw/golf-vi/golf-2-0-tdi/golf-vi-10-08-09-12_32/kfz-steuer. Accessed: 2023-10-15.

Balac, M., Rothfeld, R.L., Horl, S., 2019. The Prospects of on-demand Urban Air Mobility in Zurich, Switzerland, in: 2019 IEEE Intelligent Transportation Systems Conference (ITSC), IEEE. pp. 906–913. doi:10.1109/ITSC.2019.8916972.

Barron, F., Barrett, B.E., 1996. The Efficacy of SMARTER — Simple Multi-Attribute Rating Technique Extended to Ranking. Acta Psychologica 93, 23–36. doi:10.1016/0001-6918(96)00010-8.

Beyne, E.E., Castro, S.G., 2022. Preliminary Performance Assessment of a Long-Range eVTOL Aircraft, in: AIAA SCITECH 2022 Forum, American Institute of Aeronautics and Astronautics, San Diego, CA & Virtual. p. 1030. doi:10.2514/6.2022-1030.

Birge, J.R., Louveaux, F., 2011. Introduction to Stochastic Programming. Springer Series in Operations Research and Financial Engineering, Springer New York. doi:10.1007/978-1-4614-0237-4.

Bissel, M., 2023. A Public Transport Ticket that Moved a Country: Assessing the Value of the German 9-Euro-Ticket as a Socio-Technical Experiment. Findings doi:10.32866/001c.84645.

Biswas, S., Anavatti, S.G., Garratt, M.A., 2021. Path Planning and Task Assignment for Multiple UAVs in Dynamic Environments, in: Unmanned Aerial Systems. Elsevier, pp. 81–102. doi:10.1016/B978-0-12-820276-0.00011-X.

Boo, J., Lee, S.Y., Song, B.D., 2023. The UAM Service Network: Multi-Objective and Multi-Period Design for UAM Airports. Asia Pacific Journal of Marketing and Logistics doi:10.1108/APJML-03-2022-0257.

Brulin, S., Olhofer, M., 2023. Bi-level Network Design for UAM Vertiport Allocation Using Activity-Based Transport Simulations, in: 6th International Electric Vehicle Technology Conference 2023 (EVTeC), arXiv. doi:10.48550/ARXIV.2307.14731.

Bulusu, V., Onat, E.B., Sengupta, R., Yedavalli, P., Macfarlane, J., 2021. A Traffic Demand Analysis Method for Urban Air Mobility. IEEE Transactions on Intelligent Transportation Systems 22, 6039–6047. doi:10.1109/TITS.2021.3052229.

Bundesamt fuer Jusitz, 2015. Luftverkehrs-Ordnung (LuftVO).

Campbell, J.F., 1994. Integer Programming Formulations of Discrete Hub Location Problems. European Journal of Operational Research 72, 387–405. doi:10.1016/0377-2217(94)90318-2.

Campbell, J.F., 1996. Hub Location and the *p* -Hub Median Problem. Operations Research 44, 923–935. doi:`10.1287/opre.44.6.923`.

Cullinane, S., 2002. The Relationship between Car Ownership and Public Transport Provision: A Case Study of Hong Kong. Transport Policy 9, 29–39. doi:`10.1016/S0967-070X(01)00028-2`.

Damart, S., Roy, B., 2009. The Uses of Cost–Benefit Analysis in Public Transportation Decision-Making in France. Transport Policy 16, 200–212. doi:`10.1016/j.tranpol.2009.06.002`.

Daskilewicz, M., German, B., Warren, M., Garrow, L.A., Boddupalli, S.S., Douthat, T.H., 2018. Progress in Vertiport Placement and Estimating Aircraft Range Requirements for eVTOL Daily Commuting, in: 2018 Aviation Technology, Integration, and Operations Conference, American Institute of Aeronautics and Astronautics. p. 2884. doi:`10.2514/6.2018-2884`.

Doole, M.M., Ellerbroek, J., Hoekstra, J.M., 2018. Drone Delivery: Urban Airspace Traffic Density Estimation. 8th SESAR Innovation Days, 2018 .

Easterlin, R.A., 2005. Diminishing Marginal Utility of Income? Caveat Emptor. Social Indicators Research 70, 243–255. doi:`10.1007/s11205-004-8393-4`.

Fadhil, D.N., 2018. A GIS-based Analysis for Selecting Ground Infrastructure Locations for Urban Air Mobility. Master's thesis. Technical University of Munich.

Farahani, R.Z., Hekmatfar, M., Arabani, A.B., Nikbakhsh, E., 2013. Hub Location Problems: A Review of Models, Classification, Solution Techniques, and Applications. Computers & Industrial Engineering 64, 1096–1109. doi:`10.1016/j.cie.2013.01.012`.

Fleetcor, 2023. Aktuelle Kraftstoffpreise für Diesel und Benzin. https://fleetcor.de/dienstleistungen/fleetcor-preisvergleich.

Geoffrion, A.M., 1972. Generalized Benders Decomposition. Journal of Optimization Theory and Applications 10, 237–260. doi:`10.1007/BF00934810`.

Geurs, K.T., Van Wee, B., 2004. Accessibility Evaluation of Land-Use and Transport Strategies: Review and Research Directions. Journal of Transport Geography 12, 127–140. doi:`10.1016/j.jtrangeo.2003.10.005`.

Goel, V., Grossmann, I.E., 2006. A Class of Stochastic Programs with Decision Dependent Uncertainty. Mathematical Programming 108, 355–394. doi:`10.1007/s10107-006-0715-7`.

Gunady, N., Sells, B.E., Patel, S.R., Chao, H., DeLaurentis, D.A., Crossley, W.A., 2022. Evaluating Future Electrified UAM-Enabled Middle-Mile Cargo Delivery Operations, in: AIAA AVIATION 2022 Forum, American Institute of Aeronautics and Astronautics. p. 3756. doi:`10.2514/6.2022-3756`.

Guo, T., Wu, H., Antoniou, C., 2024. Impact of UAM Sitting on Travel Time Savings and Accessibility Improvements: A Case Study of Munich Metropolitan Area. Presented in the 103rd Transportation Research Board (TRB) Annual Meeting, Washington, DC, Jan 7-11 doi:`10.2139/ssrn.4484698`.

Han, D., Lee, J.H., 2021. Two-Stage Stochastic Programming Formulation for Optimal Design and Operation of Multi-Microgrid System Using Data-Based Modeling of Renewable Energy Sources. Applied Energy 291, 116830. doi:`10.1016/j.apenergy.2021.116830`.

Hanna, R., Kreindler, G., Olken, B.A., 2017. Citywide Effects of High-Occupancy Vehicle Restrictions: Evidence from "Three-in-One" in Jakarta. Science 357, 89–93. doi:`10.1126/science.aan2747`.

He, M., Sun, B., Liu, Z., Garikapati, V., Wang, Q., Ge, Y., Hoshiko, J., 2023. A Hierarchical Optimization Method (Home) for Vertiport Siting. Preprint. SSRN. doi:`10.2139/ssrn.4385974`.

Held, M., Rosat, N., Georges, G., Pengg, H., Boulouchos, K., 2021. Lifespans of Passenger Cars in Europe: Empirical Modelling of Fleet Turnover Dynamics. European Transport Research Review 13, 9. doi:`10.1186/s12544-020-00464-0`.

Holden, J., Goel, N., 2016. Fast-Forwarding to a Future of On-Demand Urban Air Transportation. Technical Report. Uber Elevate.

Horni, A., Nagel, K., Axhausen, K.W., 2016. The Multi-Agent Transport Simulation MATSim. Ubiquity Press. doi:`10.5334/baw`.

Husemann, M., Lahrs, L., Stumpf, E., 2023. The Impact of Dispatching Logic on the Efficiency of Urban Air Mobility Operations. Journal of Air Transport Management 108, 102372. doi:`10.1016/j.jairtraman.2023.102372`.

Immoportal, 2023. Grundsütckspreise nach Städten | immoportal.com. https://www.immoportal.com/grundstueckspreise. Accessed: 2023-10-21.

Infanger, G., 1992. Monte Carlo (Importance) Sampling within a Benders Decomposition Algorithm for Stochastic Linear Programs. Annals of Operations Research 39, 69–95. doi:`10.1007/BF02060936`.

infas, DLR, IVT, 360, I., 2020. Mobilität in Deutschland—MiD, Regionalbericht Stadt München, Münchner Umland Und MVV-Verbundraum. Studie von Infas, DLR, IVT Und Infas 360 Im Auftrag Des Bundesministeriums Für Verkehr Und Digitale Infrastruktur (FE-Nr. 70.904/15). Technical Report. Bundesministeriums fuer Verkehr und digital Infrastruktur.

Jeong, J., So, M., Hwang, H.Y., 2021. Selection of Vertiports Using K-Means Algorithm and Noise Analyses for Urban Air Mobility (UAM) in the Seoul Metropolitan Area. Applied Sciences 11, 5729. doi:`10.3390/app11125729`.

Karowski, S., 2023. Statt Zehnfacher Erhöhung: Anwohnerparken in München Kostet weiter 30 Euro im Jahr. https://www.merkur.de/lokales/muenchen/freistaat-lehnt-erhoehung-ab-anwohnerparken-in-muenchen-kostet-weiter-30-euro-im-jahr-92039842.html. Accessed: 2023-11-04.

Kellermann, R., Biehle, T., Fischer, L., 2020. Drones for Parcel and Passenger Transportation: A Literature Review. Transportation Research Interdisciplinary Perspectives 4, 100088. doi:`10.1016/j.trip.2019.100088`.

Li, A., Hansen, M., Zou, B., 2022. Traffic Management and Resource Allocation for UAV-based Parcel Delivery in Low-Altitude Urban Space. Transportation Research Part C: Emerging Technologies 143, 103808. doi:`10.1016/j.trc.2022.103808`.

Lim, E., Hwang, H., 2019. The Selection of Vertiport Location for On-Demand Mobility and Its Application to Seoul Metro Area. International Journal of Aeronautical and Space Sciences 20, 260–272. doi:`10.1007/s42405-018-0117-0`.

Lin, M.C., Wang, C.C., Chen, M.S., Chang, C.A., 2008. Using AHP and TOPSIS Approaches in Customer-Driven Product Design Process. Computers in Industry 59, 17–31. doi:`10.1016/j.compind.2007.05.013`.

Liu, Y., Lyu, C., Bai, F., Parishwad, O., Li, Y., 2023. The Role of Intelligent Technology in the Development of Urban Air Mobility Systems: A Technical Perspective. Fundamental Research , S2667325823002418doi:`10.1016/j.fmre.2023.08.006`.

Lloyd-Williams, H., Lloyd-Williams, H., 2019. The Role of Multi-Criteria Decision Analysis (MCDA) in Public Health Economic Evaluation. Applied Health Economics for Public Health Practice and Research , 301–311doi:`10.1093/med/9780198737483.003.0013`.

Lu, C., Maciejewski, M., Wu, H., Nagel, K., 2023. Demand-Responsive Transport for Students in

Rural Areas: A Case Study in Vulkaneifel, Germany. Transportation Research Part A: Policy and Practice 178, 103837. doi:`10.1016/j.tra.2023.103837`.

Lu, Q.L., Qurashi, M., Antoniou, C., 2024. A two-stage Stochastic Programming Approach for Dynamic OD Estimation Using LBSN Data. Transportation Research Part C: Emerging Technologies 158, 104460. URL: `https://www.sciencedirect.com/science/article/pii/S0968090X23004503`, doi:`https://doi.org/10.1016/j.trc.2023.104460`.

Malaek, S.M.B., Rassouli, F., S. Reza Fattahi, M., Yasamin Karamian, Alireza Akbari, Akbari, H., Alizadeh, M., 2019. SPRICHO; An On-demand Energy-efficient E-VTOL Airtaxi. Technical Report. Sharif University of Technology.

Meyer, M.D., 1999. Demand Management as an Element of Transportation Policy: Using Carrots and Sticks to Influence Travel Behavior. Transportation Research Part A: Policy and Practice 33, 575–599. doi:`10.1016/S0965-8564(99)00008-7`.

Mirchandani, P., Head, L., 2001. A Real-Time Traffic Signal Control System: Architecture, Algorithms, and Analysis. Transportation Research Part C: Emerging Technologies 9, 415–432. doi:`10.1016/S0968-090X(00)00047-4`.

Moeckel, R., Kuehnel, N., Llorca, C., Moreno, A.T., Rayaprolu, H., 2020. Agent-Based Simulation to Improve Policy Sensitivity of Trip-Based Models. Journal of Advanced Transportation 2020, 1–13. doi:`10.1155/2020/1902162`.

Moreno, C., Allam, Z., Chabaud, D., Gall, C., Pratlong, F., 2021. Introducing the "15-Minute City": Sustainability, Resilience and Place Identity in Future Post-Pandemic Cities. Smart Cities 4, 93–111. doi:`10.3390/smartcities4010006`.

Ning, C., You, F., 2019. Optimization under Uncertainty in the Era of Big Data and Deep Learning: When Machine Learning Meets Mathematical Programming. Computers & Chemical Engineering 125, 434–448. doi:`10.1016/j.compchemeng.2019.03.034`.

O'kelly, M.E., 1987. A Quadratic Integer Program for the Location of Interacting Hub Facilities. European Journal of Operational Research 32, 393–404. doi:`10.1016/S0377-2217(87)80007-3`.

Onat, E.B., Bulusu, V., Chakrabarty, A., Hansen, M., Sengupta, R., Sridar, B., 2023. Evaluating eVTOL Network Performance and Fleet Dynamics through Simulation-Based Analysis, in: AIAA SciTech Forum 2024, arXiv. p. 0336. doi:`10.48550/ARXIV.2312.02505`.

Otte, T., Metzner, N., Lipp, J., Schwienhorst, M.S., Solvay, A.F., Meisen, T., 2018. User-centered Integration of Automated Air Mobility into Urban Transportation Networks, in: 2018 IEEE/AIAA 37th Digital Avionics Systems Conference (DASC), IEEE. pp. 1–10. doi:`10.1109/DASC.2018.8569820`.

Patterson, M.D., Antcliff, K.R., Kohlman, L.W., 2018. A Proposed Approach to Studying Urban Air Mobility Missions Including an Initial Exploration of Mission Requirements, in: Annual Forum and Technology Display.

Pereira, M.V.F., Pinto, L.M.V.G., 1991. Multi-Stage Stochastic Optimization Applied to Energy Planning. Mathematical Programming 52, 359–375. doi:`10.1007/BF01582895`.

Ploetner, K.O., Al Haddad, C., Antoniou, C., Frank, F., Fu, M., Kabel, S., Llorca, C., Moeckel, R., Moreno, A.T., Pukhova, A., Rothfeld, R., Shamiyeh, M., Straubinger, A., Wagner, H., Zhang, Q., 2020. Long-Term Application Potential of Urban Air Mobility Complementing Public Transport: An Upper Bavaria Example. CEAS Aeronautical Journal 11, 991–1007. doi:`10.1007/s13272-020-00468-5`.

Pukhova, A., Llorca, C., Moreno, A., Staves, C., Zhang, Q., Moeckel, R., 2021. Flying Taxis Revived: Can Urban Air Mobility Reduce Road Congestion? Journal of Urban Mobility 1, 100002. doi:`10.1016/j.urbmob.2021.100002`.

Rahimian, H., Mehrotra, S., 2019. Distributionally Robust Optimization: A Review. arXiv preprint arXiv:1908.05659 doi:`10.48550/ARXIV.1908.05659`.

Rajendran, S., Srinivas, S., 2020. Air Taxi Service for Urban Mobility: A Critical Review of Recent Developments, Future Challenges, and Opportunities. Transportation Research Part E: Logistics and Transportation Review 143, 102090. doi:`10.1016/j.tre.2020.102090`.

Rath, S., Chow, J.Y.J., 2022. Air Taxi Skyport Location Problem with Single-Allocation Choice-Constrained Elastic Demand for Airport Access. Journal of Air Transport Management 105, 102294.

Rockafellar, R.T., Wets, R.J.B., 1991. Scenarios and Policy Aggregation in Optimization Under Uncertainty. Mathematics of Operations Research 16, 119–147. doi:`10.1287/moor.16.1.119`.

Rothfeld, R., Fu, M., Balać, M., Antoniou, C., 2021. Potential Urban Air Mobility Travel Time Savings: An Exploratory Analysis of Munich, Paris, and San Francisco. Sustainability 13, 2217. doi:`10.1136/bmj.307.6909.924`.

Rothfeld, R.L., 2021. Agent-Based Modelling and Simulation of Urban Air Mobility Operation. Ph.D. thesis. Technical University of Munich.

Schweiger, K., Preis, L., 2022. Urban Air Mobility: Systematic Review of Scientific Publications and Regulations for Vertiport Design and Operations. Drones 6, 179. doi:`10.3390/drones6070179`.

Shamiyeh, M., Rothfeld, R., Mirko, H., 2018. A Performance Benchmark of Recent Personal Air Vehicle Concepts for Urban Air Mobility, in: The 31st Congress of the International Council of the Aeronautical Sciences, p. 10.

Sparkasse, 2023. Privatkredit Günstig Online Beantragen | Stadtsparkasse München. https://www.sskm.de/de/home/produkte/kredite/sparkassen-privatkredit.html? Accessed: 2023-11-16.

Statista, 2022. Building Materials Price Growth Germany 2022, by Type. https://www.statista.com/statistics/1378439/annual-price-change-of-construction-materials-germany-by-material/. Accessed: 2023-12-05.

Statistia, 2023. Häufigkeit der Autowäsche in Deutschland 2019. https://de.statista.com/statistik/daten/studie/36621/umfrage/haeufigkeit-der-autowaesche-in-deutschland/. Accessed: 2023-11-16.

Straubinger, A., Verhoef, E., de Groot, H.L., 2021. Will Urban Air Mobility Fly? The Efficiency and Distributional Impacts of UAM in Different Urban Spatial Structures. Transportation Research Part C Emerging Technologies 127. doi:`10.1016/j.trc.2021.103124`.

Swaminathan, N., Reddy, S.R.P., RajaShekara, K., Haran, K.S., 2022. Flying Cars and eV-TOLs—Technology Advancements, Powertrain Architectures, and Design. IEEE Transactions on Transportation Electrification 8, 4105–4117. doi:`10.1109/TTE.2022.3172960`.

Syed, N., Rye, M., Ade, M., Trani, A., Hinze, N., Swingle, H., Smith, J.C., Dollyhigh, S., Marien, T., 2017. Preliminary Considerations for ODM Air Traffic Management based on Analysis of Commuter Passenger Demand and Travel Patterns for the Silicon Valley Region of California, in: 17th AIAA Aviation Technology, Integration, and Operations Conference, American Institute of Aeronautics and Astronautics. p. 3082. doi:`10.2514/6.2017-3082`.

Technische Hochschule Ingolstadt, 2022. AMI-AirShuttle - Holistische Air Mobility Initiative Bayern. `https://hcig.thi.de/project/ami-airshuttle/`. Accessed: 2024-01-12.

The World Bank, 2022. WDI - The World by Income and Region. https://datatopics.worldbank.org/world-development-indicators/the-world-by-income-and-region.html. Accessed: 2023-09-23.

Triantaphyllou, E., Shu, B., Sanchez, S.N., Ray, T., 1998. Multi-Criteria Decision Making: an Operations Research Approach. Encyclopedia of electrical and electronics engineering 15, 175–186.

Tuchen, S., LaFrance-Linden, D., Hanley, B., Lu, J., McGovern, S., Litvack-Winkler, M., 2022. Urban Air Mobility (UAM) and Total Mobility Innovation Framework and Analysis Case Study: Boston Area Digital Twin and Economic Analysis, in: 2022 IEEE/AIAA 41st Digital Avionics Systems Conference (DASC), IEEE. pp. 1–14.

Vascik, P., 2017. Systems-Level Analysis of On Demand Mobility for Aviation. Master's thesis. Massachusetts Institute of Technology.

Volkswagen, 2023. Golf. https://www.volkswagen-newsroom.com/en/golf-3508. Accessed: 2023-12-05.

Wang, K., Jacquillat, A., Vaze, V., 2022. Vertiport Planning for Urban Aerial Mobility: An Adaptive Discretization Approach. Manufacturing & Service Operations Management 24, 3215–3235. doi:10.1287/msom.2022.1148.

Wang, K., Qu, X., 2023. Urban Aerial Mobility: Reshaping the Future of Urban Transportation. The Innovation 4, 100392. doi:10.1016/j.xinn.2023.100392.

Willey, L.C., Salmon, J.L., 2021. A Method for Urban Air Mobility Network Design Using Hub Location and Subgraph Isomorphism. Transportation Research Part C: Emerging Technologies 125, 102997. doi:10.1016/j.trc.2021.102997.

Wu, Z., Zhang, Y., 2021. Integrated Network Design and Demand Forecast for On-Demand Urban Air Mobility. Engineering 7, 473–487. doi:10.1016/j.eng.2020.11.007.

Zeng, B., Zhao, L., 2013. Solving Two-Stage Robust Optimization Problems Using a Column-and-Constraint Generation Method. Operations Research Letters 41, 457–461. doi:10.1016/j.orl.2013.05.003.